Phys. Lett. B 871 (2025) 139970

Contents lists available at ScienceDirect

Physics Letters B

journal homepage: www.elsevier.com/locate/physletb

Letter

Directed and elliptic flow observations in Sn+Sn collisions with radioactive beams at 270 MeV/u

M. Kurata-Nishimura [a,*], M. Kaneko [a,b], T. Isobe [a], T. Murakami [b], A. Ono [c,a], N. Ikeno [d,a], C. Y. Tsang [e,f], J. Barney [e,f], J. Estee [e,f], G. Jhang [e], J. W. Lee [g], W. G. Lynch [e,f], M. B. Tsang [e,f], R. Shane [e], C. Santamaria [e], S. Tangwancharoen [f,h,i], R. Wang [e], A. B. McIntosh [j], S. J. Yennello [j,k], G. Cerizza [e], J. Manfredi [e,f], P. Morfouace [e], P. Lasko [l], J. Łukasik [m], A. Sochocka [l], Y. J. Kim [n], P. Pawłowski [m], K. Pelczar [l], J. Brzychczyk [l], Y. Zhang [o,p], B. Hong [g], Z. G. Xiao [o], L. Atar [q,r], T. Aumann [q,r], K. Boretzky [r], I. Gasparic [s,a,q], A. Horvat [q,r], Y. Leifels [r], D. Rossi [q,r], H. Scheit [q], H. Simon [r], A. Snoch [t], H. Törnqvist [q,r], D. S. Ahn [a,u], H. Baba [a], N. Chiga [a], N. Fukuda [a], K. Ieki [v], N. Inabe [a], T. Kobayashi [c], Y. Kondo [w,a], H. S. Lee [n], T. Nakamura [w], N. Nakatsuka [a,b], S. Nishimura [a], H. Otsu [a], H. Sakurai [a], H. Sato [a], Y. Shimizu [a], T. Sumikama [a], D. Suzuki [a], H. Suzuki [a], H. Takeda [a], Y. Togano [a]

[a] *RIKEN Nishina Center, Hirosawa 2-1, Wako, Saitama, 351-0198, Japan*
[b] *Department of Physics, Kyoto University, Kita-shirakawa, Kyoto, 606-8502, Japan*
[c] *Department of Physics, Tohoku University, Sendai, 980-8578, Japan*
[d] *Department of Agricultural, Life and Environmental Sciences, Tottori University, Tottori, 680-8551, Japan*
[e] *Facility for Rare Isotope Beams, Michigan State University, East Lansing, MI, 48824, USA*
[f] *Department of Physics, Michigan State University, East Lansing, MI, 48824, USA*
[g] *Department of Physics, Korea University, Seoul, 02841, Republic of Korea*
[h] *Department of Physics, Faculty of Science, King Mongkut's University of Technology Thonburi, Bangkok, 10140, Thailand*
[i] *Center of Excellence in Theoretical and Computational Science (TACS-CoE), Faculty of Science, King Mongkut's University of Technology Thonburi, Bangkok, 10140, Thailand*
[j] *Cyclotron Institute, Texas A&M Universitycity, TX, 77843, USA*
[k] *Department of Chemistry, Texas A&M University, College Station, TX, 77843, USA*
[l] *Faculty of Physics, Astronomy and Applied Computer Science, Jagiellonian University, Pl-30-348, Krakow, Poland*
[m] *Institute of Nuclear Physics PAN, ul., Radzikowskiego 152, Krakow, 31-342, Poland*
[n] *Rare Isotope Science Project, Institute for Basic Science, 55 Expo-ro, Yuseong-gu, Daejeon, 34126, Republic of Korea*
[o] *Department of Physics, Tsinghua University, Beijing, 100084, China*
[p] *School of Physics and Technology, Nanjing Normal University, Nanjing, 210023, China*
[q] *Institut für Kernphysik, Technische Universität Darmstadt, D-64289, Darmstadt, Germany*
[r] *GSI, Helmholtzzentrum für Schwerionenforschung GmbH, D-64291, Darmstadt, Germany*
[s] *Division of Experimental Physics, Rudjer Boskovic Institute, HR-10002, Zagreb, Croatia*
[t] *Nikhef National Institute for Subatomic Physics, Amsterdam, The Netherlands*
[u] *Center for Exotic Nuclear Studies, Institute for Basic Science, Daejeon, 34126, Republic of Korea*
[v] *Department of Physics, Rikkyo University, Nishi-Ikebukuro 3-34-1, Tokyo, 171-8501, Japan*
[w] *Department of Physics, Institute of Science Tokyo, Tokyo, 152-8551, Japan*

ARTICLE INFO

Editor: B. Blank

Keywords:
Collective flow
Radioactive heavy ion collision
Isospin symmetry energy
Momentum dependent mean field potential

ABSTRACT

Radioactive tin beams were used to explore the flow observables under varying isospin asymmetries while maintaining a constant total charge. The rapidity dependence of directed flow (v_1) and elliptic flow (v_2) was studied for protons, deuterons, tritons, ^{3}He, and ^{4}He, produced in neutron-rich ^{132}Sn + ^{124}Sn and neutron-deficient ^{108}Sn + ^{112}Sn collisions at 270 MeV/nucleon. In general, heavier particles exhibited larger v_1 and v_2 values. The experimental data was used to test transport models which simulate heavy ion collisions. Specifically, comparisons were made with Antisymmetrized Molecular Dynamics (AMD) model calculations, which explicitly account for cluster correlations. Two types of momentum-dependent mean field potentials were tested. The results reveal that both v_1 and v_2 values are enhanced when the mean field incorporates stronger momentum dependence. In addition, v_2 exhibits larger sensitivity to symmetry energy than v_1 but the overall sensitivity to symmetry energy is low. In an attempt to describe the data, different parameter sets have been tried. Most describe either the hydrogen flow or helium flow reasonably well but none describes the flow of all particles simultaneously.

Available online 25 October 2025

1. Introduction

Determination of the nuclear equation of state for nuclear matter has been a significant objective for both the nuclear physics and nuclear astrophysics communities [1]. Recent advances in astronomical observations of neutron stars, such as the detection of gravitational waves (GW) from binary neutron star mergers by LIGO-Virgo detector network [2–4] and neutron star mass-radius correlation measurements from the NICER collaboration [5], have brought renewed attention and excitement to the importance of the nuclear equation of state (EOS) in physics.

Recent attempts to extract the nuclear EOS by combining the constraints from both the terrestrial experiments and the astrophysical observations [6–8] suggest that the laboratory constraints around 1.5 times the nuclear saturation density carry significant uncertainties. Reducing these uncertainties, whether through improvements in theoretical models or by increasing the accuracy of the measured data, including new measurements, is crucial for refining the equation of state for both nuclear and neutron star matter.

In the laboratory, heavy ion collisions (HICs) have been employed worldwide to investigate the nuclear EOS, as they provide a unique tool for exploring the properties of nuclear matter at densities away from nuclear saturation [9]. Furthermore, radioactive ion beam (RIB) factories offer new opportunities to study nuclear matter with high isospin asymmetry, using ion beams beyond the nuclear stability [10,11]. However, to extract meaningful physics information, such as the nuclear EOS parameters, transport models are required to simulate the dynamics of heavy ion collisions. Due to technical difficulties, very few models contain all the physics ingredients to simulate the nuclear collisions [12]. Specifically, most transport models do not contain rigorous cluster formation, which may affect the extraction of the equation of state parameters.

The collective flow has been studied as one of the most sensitive observables of the nuclear EOS [13–15] and provides information about the dynamics of heavy ion collisions. This paper presents the directed and elliptic flow measurements for light charged particles emitted in Sn+Sn reactions at 270 MeV/nucleon. The results are compared with the Antisymmetrized Molecular Dynamics (AMD) model simulations [16]. Unlike other transport models that rely solely on mean field propagation of nucleons and nucleon-nucleon collisions, the AMD model incorporates cluster correlations during the dynamical evolution of heavy ion collisions, offering a more comprehensive treatment of cluster formation [17,18]. Furthermore, we take advantage of the most recent version of the AMD that allows varying the momentum-dependent interaction of the mean field, which has been shown to influence the flow observable [19].

2. Experiment

Radioactive ion (RI) beams allow the investigation of isospin symmetry energy directly by providing exotic projectiles with very different neutron-excess contents. This experiment was performed at RI Beam Factory operated by RIKEN Nishina Center and CNS, University of Tokyo. A heavy ion collision experiment using the RI beams were conducted with the SAMURAI Pion Reconstruction and Ion-Tracker Time Projection Chamber (SπRIT-TPC) located in the SAMURAI experimental area [20,21]. In this paper, the data were obtained from the reactions of a neutron-rich system ^{132}Sn + ^{124}Sn and a system which is nearly symmetric ^{108}Sn + ^{112}Sn at an incident energy of 270 MeV/u. The ^{132}Sn and ^{108}Sn secondary beams were separated using BigRIPS [22] and directed onto enriched targets of ^{124}Sn (608 mg/cm^2) and ^{112}Sn (561 mg/cm^2). At the midpoint of the target, the beam energy was 268 MeV/u. The typical beam intensity was $7.5 \sim 9.5 \times 10^3$ particles per second, with beam purities of 54% for ^{132}Sn beam and 52% for ^{108}Sn beam. While low-Z contaminants were present, they contributed less than 1% to the overall statistics. In this study, a total of 2.5 million and 1.5 million events were analyzed for the reactions ^{132}Sn + ^{124}Sn and ^{108}Sn + ^{112}Sn, respectively.

The experimental setup and detector configurations are described in detail in Refs. [23–26]. The ^{124}Sn and ^{112}Sn solid targets were placed 15 mm upstream of the SπRIT-TPC entrance window. Electrons ionized by charged particles passing through the SπRIT-TPC were drifted upward and then amplified in a field cage. Energy deposits along each particle path were measured by pads located on a top plate. Track reconstruction was performed by associating amount of charge and hit timing on pads. A helical track based on the Riemann fit [27] was utilized to evaluate the magnetic rigidity of each track. light charged particles were well separated [26,28,29] by adopting dedicated software to compensate for electronic saturation [30], and space charge corrections [31]. The multiplicity (M) of each event was determined by the number of reconstructed tracks originating from the vertex within 20 mm for all charged particles including pions. In this paper, mid-central collisions were chosen within $47 \leq \mathrm{M} \leq 56$ for ^{132}Sn + ^{124}Sn collisions and $46 \leq \mathrm{M} \leq 55$ for ^{108}Sn + ^{112}Sn collisions, which corresponded to $0.15 \leq b_0 \leq 0.35$ with the reduced impact parameter (b_0) determined in Ref. [28].

In this study, we required at least 15 clustered pads and a vertex in the beam axis within 4.0 mm to select reliable tracks. For those tracks, particle identification was applied depending on the correlation between the mean energy loss per unit length along the path and its magnetic rigidity. Proton, deuteron, triton, ^{3}He, and ^{4}He were separated in the following analysis.

In the flow analysis, the reaction plane was determined using charged particles with mass number $1 \leq A \leq 4$ detected within the TPC's geometrical acceptance. However, the flow observable values were determined only with particles accepted within the range of $(-20° < \phi < 30°) \cup (160° < \phi) \cup (\phi < -150°)$ where the tracks are of good quality. The acceptance represented by the mass invariant plots of transverse momentum vs. the scaled rapidity for p, d, t, ^{3}He, and ^{4}He, is illustrated in Fig. 1. Here, the horizontal axis indicates scaled rapidity, $y/y^{\mathrm{cm}}_{\mathrm{NN}} - 1$, where y is the rapidity of the detected particle in the laboratory frame and the $y^{\mathrm{cm}}_{\mathrm{NN}}$ is the rapidity of the nucleon-nucleon (NN) center-of-mass in the laboratory frame. To reduce the impact of contamination from triton on ^{3}He, the systematic error was minimized by limiting the acceptance of these particles to within the scaled rapidity $y/y^{\mathrm{cm}}_{\mathrm{NN}} - 1 > -0.3$, while $y/y^{\mathrm{cm}}_{\mathrm{NN}} - 1 > -0.5$ for other particles. In the gated phase space shown in Fig. 1, a detection efficiency exceeding 90 % was achieved, covering the entire range of transverse momentum. For flow observables, efficiency corrections are not important, and they were, therefore, not taken into account.

3. AMD Model comparison

We employed the AMD model [17,32,33] to gain physics insights from the data. AMD describes the dynamics of a many-nucleon system using the time evolution of a Slater determinant of Gaussian wave packets. Two-nucleon collisions are treated as a stochastic transition from an initial state to a final state. AMD treats cluster correlations explicitly by extending the two-nucleon collision process. The details are described in Ref. [17]. Each scattered nucleon may form a cluster with surrounding particle(s) as $N_1 + N_2 + B_1 + B_2 \to C_1 + C_2$. This includes the special cases in which both or one of B_1 and B_2 is empty, e.g., $N_1 + N_2 \to N_1 + N_2$ and $N_1 + N_2 + B_1 \to C_1 + N_2$. The collision probability for a specific configuration (C_1, C_2) is expressed as

$$\frac{d\sigma(C_1, C_2)}{d\Omega} = P(C_1, C_2, p_{\mathrm{f}}, \Omega) \frac{p_{\mathrm{i}}}{v_{\mathrm{i}}} \frac{p_{\mathrm{f}}}{v_{\mathrm{f}}} |M|^2 \frac{p_{\mathrm{f}}}{p_{\mathrm{i}}}, \tag{1}$$

* Corresponding author.
E-mail address: mizuki@riken.jp (M. Kurata-Nishimura).

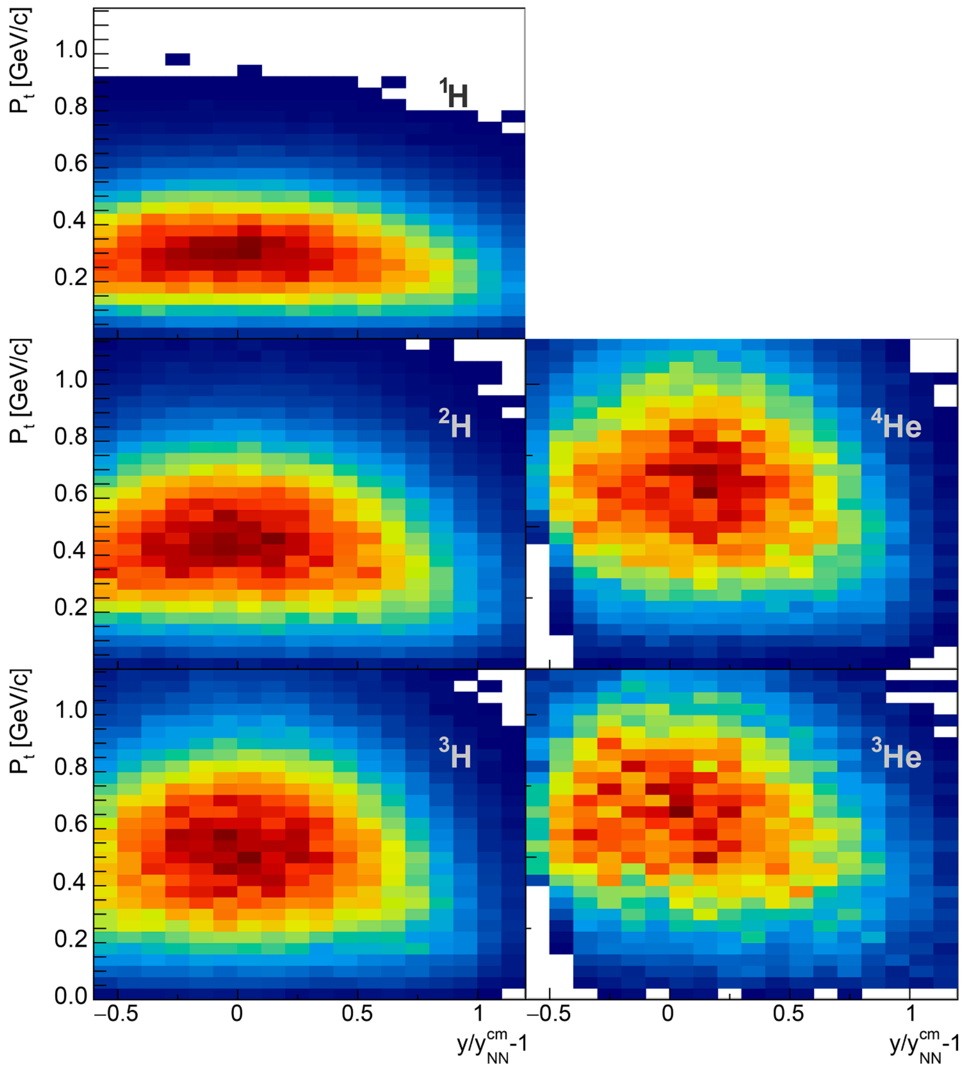

Fig. 1. The SπRIT-TPC acceptance for light charged particles for the scaled impact parameter within $0 \le b_0 \le 0.15$. The horizontal axis is the scaled rapidity, $y/y_{\mathrm{NN}}^{\mathrm{cm}} - 1$, where y is the rapidity of the detected particle in the laboratory frame and the $y_{\mathrm{NN}}^{\mathrm{cm}}$ is the rapidity of the nucleon-nucleon (NN) center-of-mass in the laboratory frame. The vertical axis corresponds to the transverse momentum. To minimize contamination from triton on ^{3}He, $y/y_{\mathrm{NN}}^{\mathrm{cm}} - 1 > -0.3$ was analyzed, while $y/y_{\mathrm{NN}}^{\mathrm{cm}} - 1 > -0.5$ for other particles.

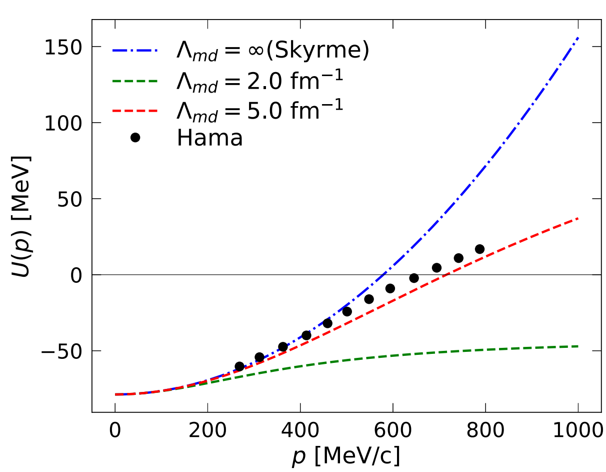

Fig. 2. The momentum-dependent mean field potential as follows: The blue dot-dashed line represents the momentum dependence in the Skyrme SLy4 interaction. The red dashed line corresponds to $\Lambda_{\mathrm{md}} = 5\ \mathrm{fm}^{-1}$ [17], where the momentum dependence was moderately weakened to be similar to the empirical optical potential described by Hama et al [36](shown with solid circles). The green dashed line indicates $\Lambda_{\mathrm{md}} = 2\ \mathrm{fm}^{-1}$, where the momentum dependence was weakened strongly. (For interpretation of the references to colour in this figure legend, the reader is referred to the web version of this article.)

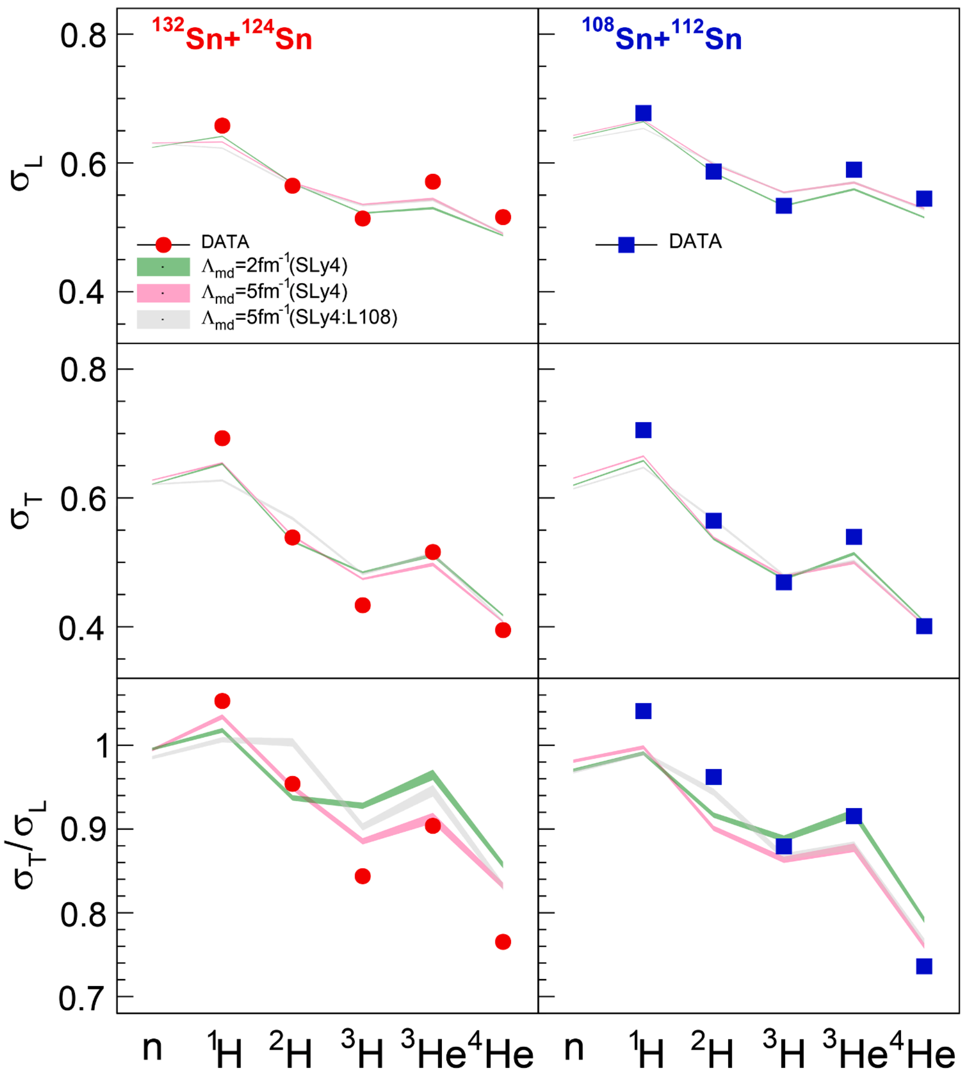

Fig. 3. The sigma values in longitudinal (TOP) and transverse (middle) rapidity distributions for $A \leq 4$. AMD with four parameter sets; $\Lambda_{\mathrm{md}} = 2\ \mathrm{fm}^{-1}$(SLy4) (green band), $\Lambda_{\mathrm{md}} = 5\ \mathrm{fm}^{-1}$(SLy4) (magenta band), and $\Lambda_{\mathrm{md}} = 5\ \mathrm{fm}^{-1}$(SLy4 : L108) (gray band) are compared with data. The details are described in the text. (For interpretation of the references to colour in this figure legend, the reader is referred to the web version of this article.)

where p_{i} and v_{i} are the initial relative momentum and the velocity between the colliding nucleons N_1 and N_2. The relative momentum vector after the momentum transfer between them is denoted by (p_{f}, Ω), and p_{f} is determined to conserve the energy E of the system which includes the adopted effective interaction. The velocity factor $v_{\mathrm{f}} = \partial E/\partial p_{\mathrm{f}}$ as a function of p_{f} also depends on the effective interaction. The overlap probability factor for cluster formation, $P(C_1, C_2, p_{\mathrm{f}}, \Omega)$, is defined by considering the non-orthogonality between the states of different configurations. Cluster breaking is treated in the same framework when N_1 or N_2 is a nucleon in a previously formed cluster.

An important input to the calculation is the matrix element $|M|^2$ for the two-nucleon scattering which may be modified in a nuclear medium. We express it as

$$|M|^2 = (2/m_N)^2 d(\tilde{\sigma}_{NN})/d\Omega, \tag{2}$$

where the effective in-medium nucleon-nucleon cross section $\tilde{\sigma}_{NN}$ is parameterized as

$$\tilde{\sigma}_{NN} = [1 + x(\rho - \rho')/\rho_0]\sigma_0 \tanh \frac{\sigma_{NN}^{(\mathrm{free})}}{\sigma_0}, \tag{3}$$

$$\sigma_0 = 0.4(\rho')^{-2/3}. \tag{4}$$

In these formulas, the right-hand side in Eq. (2) is evaluated at an average of p_{i} and p_{f}, and ρ' is a density with a momentum cut as defined by Eq. (161) in Ref. [12]. To adjust the stopping in the next section, we include a term proportional to $(\rho - \rho')/\rho_0$ where ρ is the density and $\rho_0 = 0.16\ \mathrm{fm}^{-3}$, is the saturation density.

The effective interactions used in AMD are described in Ref. [17]. The present study uses two interactions, labeled SLy4 and SLy4:L108, which differ in the density dependence of the symmetry energy. The original SLy4 interaction contains a slope parameter $L = 46$ MeV, while SLy4:L108 has $L = 108$ MeV. The original Skyrme interaction [34,35] exhibits a quadratic momentum dependence of the mean field, characterized by an effective mass $m^*/m = 0.70$ in symmetric matter at saturation density. However, this momentum dependence is too strong at high momenta (blue dot-dashed line in Fig. 2), and has been modified by introducing a momentum cutoff parameter $\Lambda_{\mathrm{md}} = 5\ \mathrm{fm}^{-1}$ in Ref. [17], to reasonably reproduce the empirical optical potential by Hama *et al.* [36], as shown in Fig. 2 by the red dashed line. To investigate the impact of the momentum dependence of the mean field on the flow observables, we compare two cases of $\Lambda_{\mathrm{md}} = 5\ \mathrm{fm}^{-1}$ and $\Lambda_{\mathrm{md}} = 2\ \mathrm{fm}^{-1}$. The latter case, which corresponds to a choice in Ref. [37], exhibits a weak momentum dependence as shown in Fig. 2 by the green dashed line.

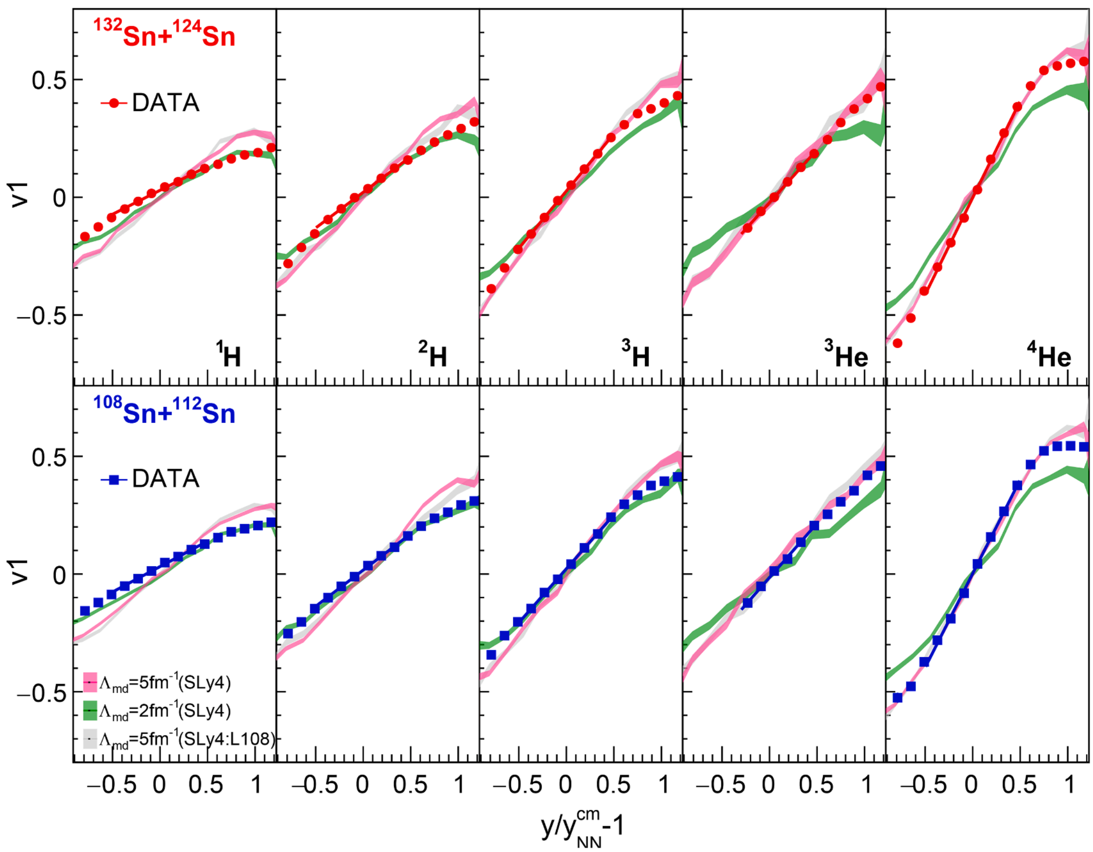

Fig. 4. The directed flow, v_1 plotted as a function of scaled rapidity. Top and bottom panels are for ^{132}Sn + ^{124}Sn and ^{108}Sn + ^{112}Sn, respectively. A linear function evaluates the slope parameter, v_{11}, fitting at the mid-rapidity. AMD calculations with $\Lambda_{\mathrm{md}} = 2\ \mathrm{fm}^{-1}$(SLy4) (green band), $\Lambda_{\mathrm{md}} = 5\ \mathrm{fm}^{-1}$(SLy4) (magenta band), and $\Lambda_{\mathrm{md}} = 5\ \mathrm{fm}^{-1}$(SLy4 : L108) (gray band) are also plotted for comparison. (For interpretation of the references to colour in this figure legend, the reader is referred to the web version of this article.)

4. Stopping analysis and results

In the heavy-ion collisions considered in this study, the AMD calculations with cluster correlations predict that the system is compressed to a maximum density of approximately $2\rho_0$ [32], after which it expands in all directions. The degree of stopping in such collisions is typically characterized by comparing the longitudinal and transverse emissions. Stopping is known to depend on several factors in transport models, such as the incompressibility and the two-nucleon collision cross sections. The incompressibility is fixed to $K = 230$ MeV in this study, while the impact of the momentum dependence of the mean field (Λ_{md}) on the stopping must be carefully considered. Specifically, varying Λ_{md} affects the cross sections defined by Eq. (1), particularly through the factors p_f/v_f and p_i/v_i, thereby influencing stopping. Since flow is already known to be highly correlated with stopping [38], it is crucial to analyze flow observables under the condition of a consistent stopping. To achieve this, we adjust the parameter x in the matrix element according to the choice of Λ_{md}, as described below.

We analyzed the stopping power from longitudinal rapidity (y_L, the same as $y/y^{\mathrm{cm}}_{\mathrm{NN}} - 1$) and transverse rapidity (y_T) distributions for central collision events ($b_0 < 0.15$). The distribution of y_L was assumed to be symmetric around $y_L = 0$, compensating for the low efficiency of the detector for $y_L < -0.5$. The distribution of y_T with a cut of $|y_L| < 0.3$ was derived from mass and transverse momentum projecting onto an arbitrary reaction plane to eliminate collective flow effects. The spreads of the y_L and y_T distributions, defined as $\sigma_{L(T)} = \sqrt{\frac{1}{N}\Sigma_i^N \left(y_{L(T)_i}\right)^2}$, were utilized to quantify the stopping power by taking the ratio σ_T/σ_L. In Fig. 3, the ratios, σ_T/σ_L as well as σ_L and σ_T are plotted for the light charged particles from ^{132}Sn + ^{124}Sn reactions (left panels) and from ^{108}Sn + ^{112}Sn reactions (right panels). For comparison, the results from AMD were analyzed in the same manner as the data. Since stopping is affected by Λ_{md}, the parameter x in $\tilde{\sigma}_{NN}$ of Eq. (3) was adjusted to keep the predicted stopping power to be consistent with the data. We adopt the values of $x = 0.1$ for $\Lambda_{\mathrm{md}} = 5\ \mathrm{fm}^{-1}$, and $x = 0$ for $\Lambda_{\mathrm{md}} = 2\ \mathrm{fm}^{-1}$. AMD calculations for $\Lambda_{\mathrm{md}} = 5\ \mathrm{fm}^{-1}$(SLy4) (magenta band), $\Lambda_{\mathrm{md}} = 2\ \mathrm{fm}^{-1}$(SLy4) (green band), and $\Lambda_{\mathrm{md}} = 5\ \mathrm{fm}^{-1}$(SLy4 : L108) (grey band) are plotted with data in Fig. 3. The trend of particle dependence and the values of σ_L, σ_T, and σ_T/σ_L are reproduced reasonably.

5. Flow analysis and results

5.1. Directed flow (v_1)

We analyze directed flow (v_1) and elliptic flow (v_2), which are defined as the coefficients of the first and second harmonics of the Fourier expansion for the distribution of the azimuthal angle, respectively. The azimuthal angle distributions of particles, $\Delta\phi = \phi - \Psi$, were obtained by rotating its azimuthal angle with respect to the reaction plane angle Ψ,

$$\frac{1}{N}\frac{dN}{d(\Delta\phi)} = 1 + 2v_1\cos(\Delta\phi) + 2v_2\cos(2\Delta\phi). \tag{5}$$

Ψ was determined as the azimuthal angle of a flow vector $\boldsymbol{Q}$ which was obtained by summing the transverse unit vector with a sign depending on the scaled rapidity [39] as

$$\boldsymbol{Q} = \sum^{A\le 4} \omega \boldsymbol{p}_t/|p_t|, \quad \omega = \begin{cases} +1 & \text{if } y/y^{\mathrm{cm}}_{\mathrm{NN}} - 1 \ge 0 \\ -1 & \text{if } y/y^{\mathrm{cm}}_{\mathrm{NN}} - 1 < 0, \end{cases} \tag{6}$$

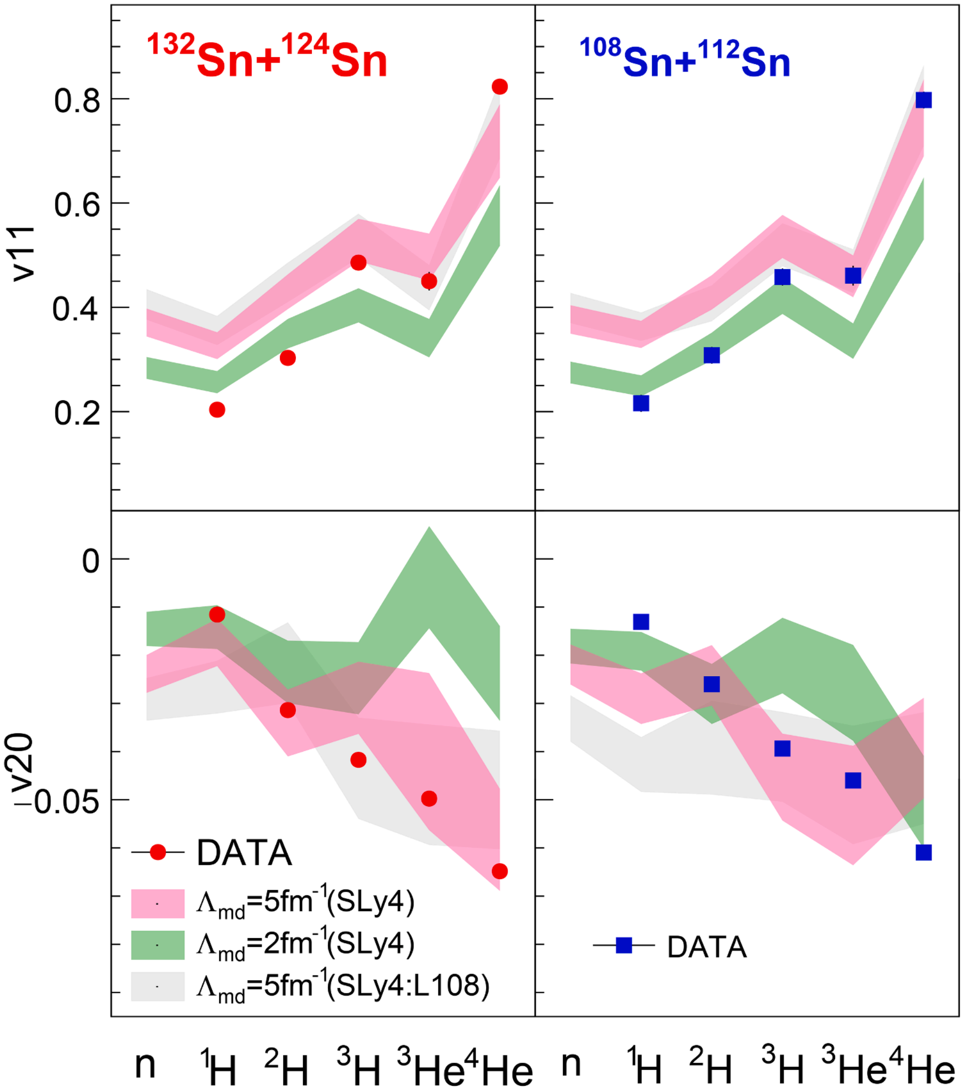

Fig. 5. Particle dependence of v_{11}, v_{20}, plotted on top and bottom, respectively. Left and right columns correspond to ^{132}Sn $+^{124}$ Sn and ^{108}Sn $+^{112}$ Sn, respectively. AMD calculations with $\Lambda_{\rm md} = 2\ {\rm fm}^{-1}$(SLy4) (green band), $\Lambda_{\rm md} = 5\ {\rm fm}^{-1}$(SLy4) (magenta band), and $\Lambda_{\rm md} = 5\ {\rm fm}^{-1}$(SLy4 : L108) (gray band) are also plotted for comparison. (For interpretation of the references to colour in this figure legend, the reader is referred to the web version of this article.)

where summation runs over all light charged particles with $1 \le A \le 4$ event by event. The selected particle was excluded from $\boldsymbol{Q}$ computation to avoid auto-correlation. Since SπRIT-TPC has a rectangular shape, the reaction plane angles were corrected using shifting and flattening methods [40] to minimize detector bias. The correction factors for the reaction plane resolution are $\langle \cos(\Delta\Psi)\rangle = 0.748 \pm 0.004$ and $\langle \cos(2\Delta\Psi)\rangle = 0.416 \pm 0.006$ [39].

The directed flow v_1 as a function of the scaled rapidity is shown in Fig. 4 for proton, deuteron, triton, ^{3}He, and ^{4}He. The top panels correspond to ^{132}Sn + ^{124}Sn, while the bottom panels correspond to ^{108}Sn + ^{112}Sn. v_1 reaches a higher value with a steeper slope for heavier particles in both systems. The AMD results with the three configurations are presented: $\Lambda_{\rm md} = 2\ {\rm fm}^{-1}$(SLy4) (green band), $\Lambda_{\rm md} = 5\ {\rm fm}^{-1}$(SLy4) (magenta band), and $\Lambda_{\rm md} = 5\ {\rm fm}^{-1}$ (SLy4:L108) (gray band). Systematically, the slopes for all particles are steeper for $\Lambda_{\rm md} = 5\ {\rm fm}^{-1}$ compared to $\Lambda_{\rm md} = 2\ {\rm fm}^{-1}$. To condense the information of v_1, a linear fit is used to extract the slope parameter, v_{11} in the mid-rapidity region. v_{11} is plotted on the top half in Fig. 5 and the shaded lines represent the AMD values. The general trend that the strength of v_{11} increases with the mass number is reproduced with all three parameter sets of AMD. However, this trend is weaker in AMD than in the experimental data, so that neither $\Lambda_{\rm md} = 2\ {\rm fm}^{-1}$ nor $\Lambda_{\rm md} = 5\ {\rm fm}^{-1}$ explain v_{11} simultaneously for all particles. Different parameter sets including using SkM* instead of Skyrme SLy4 interactions have been tested. The general conclusions are similar in that the AMD calculations reproduce the v_{11} values for either Z = 1 or for Z = 2 isotopes but not for all 5 particles.

The results of ^{3}He and ^{4}He demonstrate better agreement for $\Lambda_{\rm md} = 5\ {\rm fm}^{-1}$ in both reaction systems, while the results for proton and deuteron are overestimated. On the other hand, the weaker momentum dependence of $\Lambda_{\rm md} = 2\ {\rm fm}^{-1}$ describes the hydrogen isotopes, proton, deuteron and to a certain extent triton better. The v_{11} values are similar for the two reaction systems except for ^{3}H and ^{3}He. Experimental v_{11} values of ^{3}He seems to be smaller than that of ^{3}H in the neutron-rich system, while they are similar in the ^{108}Sn + ^{112}Sn system. AMD predicts smaller v_{11} for ^{3}He in all parameter sets. The difference of v_{11} between ^{3}H and ^{3}He flow may arise from a sensitivity to the symmetry energy.

To investigate the sensitivity of flow to symmetry energy, we compared the results of $\Lambda_{\rm md} = 5\ {\rm fm}^{-1}$ from AMD with two different symmetry energy slope parameters, $L = 46$ MeV and $L = 108$ MeV, as shown in the upper panels of Fig. 5. They do not show much difference. $\Lambda_{\rm md} = 5\ {\rm fm}^{-1}$ (SLy4 : L108) seems to suppress ^{3}He values more for the ^{132}Sn + ^{124}Sn system but the uncertainties are too large to determine the slope parameter of the symmetry energy at this moment.

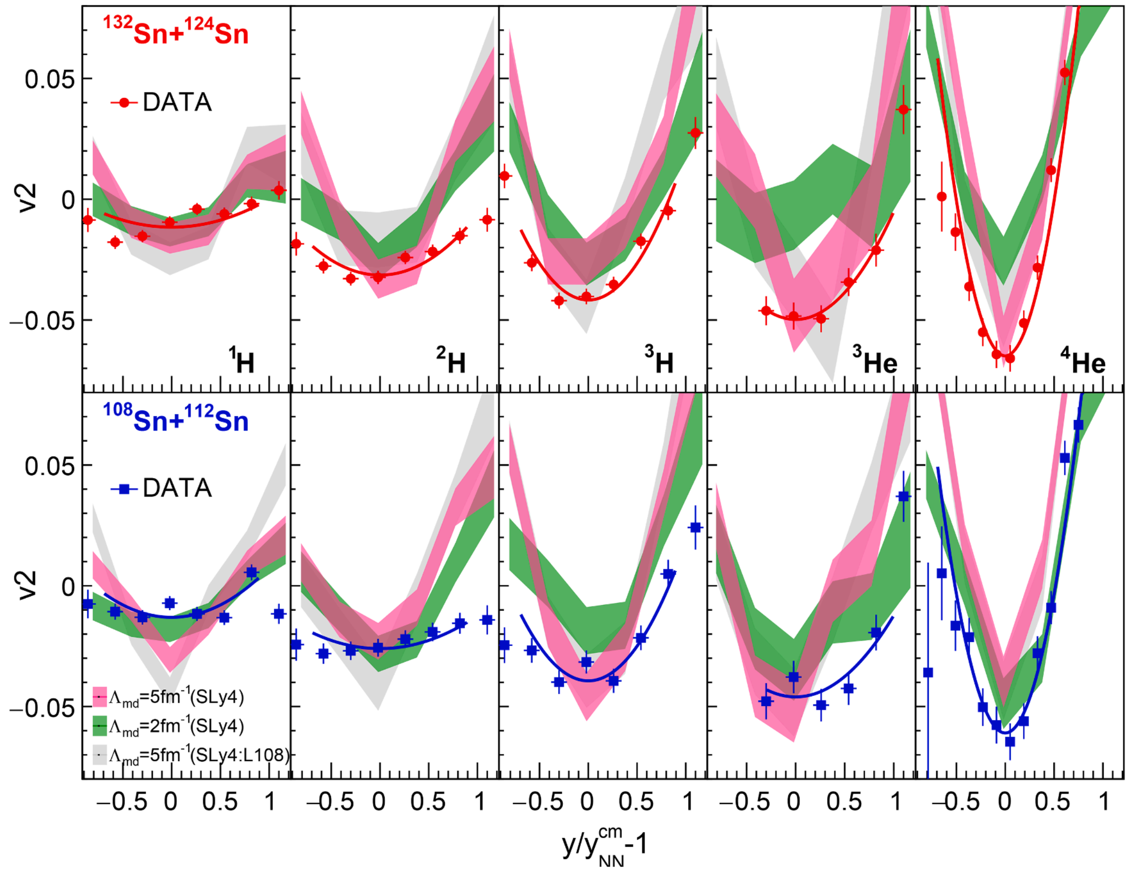

Fig. 6. The elliptic flow, v_2 plotted as a function of scaled rapidity. Top and bottom panels are for ^{132}Sn$+^{124}$Sn and ^{108}Sn$+^{112}$Sn, respectively. Solid lines in the figure show relevant results with a parabolic function, and the minimum v_2 is determined as v_{20}. AMD calculations with $\Lambda_{md} = 2\ \mathrm{fm}^{-1}$(SLy4) (green band), $\Lambda_{md} = 5\ \mathrm{fm}^{-1}$(SLy4) (magenta band), and $\Lambda_{md} = 5\ \mathrm{fm}^{-1}$(SLy4 : L108) (gray band) are also plotted for comparison. (For interpretation of the references to colour in this figure legend, the reader is referred to the web version of this article.)

5.2. Elliptic flow (v_2)

The rapidity dependence of v_2 is shown for the two systems in Fig. 6. Negative v_2 is observed, which indicates out-of-plane emission (squeeze-out) with respect to the reaction plane. The heavier particles show a more significantly negative v_2 for both systems. The strength of $|v_2|$ is influenced by several factors, including the incident energy, the size of the colliding system, and the chosen impact parameter region, as reported in Ref. [41]. Applying a low transverse momentum cut is known to enhance the results. However, this analysis does not include such a cut, as it helps compare with models.

The AMD results are displayed in the figures for the three cases in the same manner as v_1. While the calculations reproduce the overall trends of U-shape distributions, the agreement is not very good at low and high-rapidity regions. In regions of large rapidity, the contribution from spectators becomes significant during collisions with a large impact parameter. The discrepancy observed might arise from a mismatch between the experimental and calculated distributions of impact parameters. While AMD can precisely determine the impact parameter, experimental data typically encompass a broad range of impact parameters. Furthermore, it may be related to the discrepancies in the rapidity and transverse distributions between AMD and the experimental data [28,29]. To minimize the effect of impact parameter contamination, the minima of v_2 (v_{20}) were evaluated by fitting the data of each particle with a parabolic function as shown by the solid curves in Fig. 6.

The mass number dependence of $|v_{20}|$ is plotted for the two systems in the lower panels of Fig. 5. The values of $|v_{20}|$ increase monotonically with the mass and charge number. Larger $|v_{20}|$ for ^{3}He is observed than for ^{3}H. In Ref. [41], it was noticed that the elliptic flow of ^{3}H is larger than that of ^{3}He with beam energy ≥ 400 MeV/u. However, the gap between ^{3}H and ^{3}He decreases with beam energy. If we extend that dependence toward the beam energy below 400 MeV/u, it can be expected that $|v_{20}|$ for ^{3}He becomes larger than that for ^{3}H. This swapping might be linked to the turning point of the excitation function of $|v_2|$ at around 400 MeV/u [42], which is a result of the expansion speed being comparable to the crossing time of the two nuclei. The observation suggests that particles moving within the dense matter formed by heavy ion collisions are more affected by the repulsive force from the Coulomb potential when the beam energy is below 400 MeV/u. The difference between the two systems is small, but slightly larger $|v_{20}|$ is observed in ^{132}Sn + ^{124}Sn for light clusters. This might be evidence of considerable repulsive potential in the neutron-rich system.

For the AMD results, the overall $|v_{20}|$ values agree with data better if $\Lambda_{md} = 5\ \mathrm{fm}^{-1}$(SLy4) is used. The weaker momentum dependence of $\Lambda_{md} = 2\ \mathrm{fm}^{-1}$(SLy4) leads to an underestimation of the data.

In the discussions of the symmetry energy in the last subsection, there is a maximum difference of about 10 % between $L = 108$ MeV and $L = 46$ MeV settings in v_{11}. The difference is not enough to distinguish between them due to the large statistical errors. The mass dependence of v_{20} is flatter when the $L = 108$ MeV setting is used in ^{108}Sn + ^{112}Sn, and it differs by about 20 % from $L = 46$ MeV. This suggests that the mass-dependent elliptical flow may be sensitive to the symmetry energy.

6. Summary

We performed a heavy-ion collision experiment using Sn isotope beams at beam energy of 270 MeV/nucleon at the RIKEN-RIBF facility using the SπRIT-TPC detector. light charged particles with 1 ≤

$A \leq 4$ produced in the neutron-rich $^{132}Sn + ^{124}Sn$ and neutron-deficient $^{108}Sn + ^{112}Sn$ collisions were analyzed for flow and stopping observables. The rapidity dependence of the directed flow (v_1) and elliptic flow (v_2) was studied for protons, deuterons, tritons, ^{3}He, and ^{4}He, focusing on mid-central collisions within the range $0.15 \leq b_0 \leq 0.35$. To investigate the effects of the momentum-dependent mean field potential, we conducted Antisymmetrized Molecular Dynamics (AMD) model calculations that incorporates the SLy4 interactions using parameter sets with momentum dependence ($\Lambda_{md} = 5\ \mathrm{fm}^{-1}$) which is similar to the Hama potential and a weakened momentum dependence ($\Lambda_{md} = 2\ \mathrm{fm}^{-1}$). Additionally, the influence of symmetry energy was examined using a “stiff symmetry energy" parameter with slope, $L = 108$ and a “soft symmetry energy" parameter with $L = 46$ with $\Lambda_{md} = 5\ \mathrm{fm}^{-1}$.

Our findings demonstrate that the mean field potential with $\Lambda_{md} = 5\ \mathrm{fm}^{-1}$ enhances the directed flow v_1 for light charged particles compared to the weakened momentum dependence case ($\Lambda_{md} = 2\ \mathrm{fm}^{-1}$). The strength of v_1 increases with particle mass, and the particle-dependent trends of v_{11} were generally reproduced across all three parameter sets in AMD calculations. However, no parameter set fully agrees with the experimental v_{11} values for all particle species.

A negative elliptic flow (v_2), generally referred to as “squeeze-out" or “out-of-plane flow," was observed, with $|v_{20}|$ increasing monotonically with particle mass. The AMD calculations suggest that the $\Lambda_{md} = 5\ \mathrm{fm}^{-1}$ parameter set provides a good overall description of the $|v_{20}|$ values. The $\Lambda_{md} = 2\ \mathrm{fm}^{-1}$ parameter set underestimates the experimental data.

We conclude that the momentum-dependent potential influences flow observables for light charged particles, despite the AMD model predictions not aligning perfectly with the data. These results provide further insight into understanding the heavy-ion collision process.

Moreover, a notable difference was observed between ^{3}He and ^{3}H, where ^{3}He exhibited a stronger $|v_{20}|$. This observation contrasts with previous studies conducted at high beam energies (> 400 MeV/u) but aligns with expectations based on extrapolated energy dependencies below 400 MeV/u. The greater contribution of the Coulomb potential at lower beam energies likely explains this discrepancy. Our comparative analysis of the two systems indicates a slightly larger $|v_{20}|$ in $^{132}Sn + ^{124}Sn$, suggesting a stronger repulsive potential in the neutron-rich system. Additionally, a comparison of AMD calculations at $L = 46$ MeV and $L = 108$ MeV reveals that the density dependence of the symmetry energy has a relatively modest impact (approximately 10 %) on v_{11}, while the particle mass dependence of v_{20} in $^{108}Sn + ^{112}Sn$ shows a more pronounced effect (about 20 %).

This work illustrates the complex phenomena in heavy ion collisions, including the production of clusters. Those data will encourage further development of theoretical work on the collision dynamics and cluster production in heavy-ion collisions.

Data availability

Data will be made available on request.

Declaration of competing interest

The authors declare that they have no known competing financial interests or personal relationships that could have appeared to influence the work reported in this paper.

Acknowledgements

This work was supported by the Japanese MEXT KAKENHI (Grant-in-Aid for Scientific Research on Innovative Areas) grant No. 24105004, JSPS KAKENHI Nos. JP17K05432, JP19K14709, and JP21K03528, the US National Science Foundation Grant No.PHY-2209145, the U.S. Department of Energy under Grant No. DE-FG02-93ER40773, Institute for Basic Science Grant No. (IBS-R031-D1), the Polish National Science Center (NCN), Poland, under contract Nos. UMO-2013/09/B/ST2/04064 and UMO-2013/10/M/ST2/00624, the National Research Foundation of Korea (NRF) under Grant Nos. (2018R1A5A1025563 and 2013M7A1A1075764), and the Ministry of Science and Technology of China under grant No. 2022YFE0103400, Tsinghua University Initiative Scientific Research Program. I.G. was supported by HIC for FAIR and the Croatian Science Foundation under projects Nos. 1257 and 7194. One of the authors (M. K.) acknowledges support from the RIKEN Junior Research Associate Program. The computing resource for the data analysis and the theoretical calculations were provided by the HOKUSAI Great-Wave system at RIKEN. The authors also wish to thank the accelerator technical staff at RIBF for the excellent beam production. While preparing this work, the authors used Grammarly software to rectify English grammar errors. The authors have reviewed and edited the manuscript as needed and assume complete responsibility for the content of the published article. The authors thank FORTE Science Communications (https://www.forte-science.co.jp/) for English language editing.

Reference

[1] C. Aidala, A. Aprahamian, P. Bedaque, L. Bernstein, J. Carlson, M. Carpenter, K. Chipps, V. Cirigliano, I. Cloet, A. de Gouvea, R. de Souza, G. Dodge, E.J. Downie, J. Dudek, R. Fatemi, A. Gade, H. Gao, S. Gardner, S.V. Greene, A. Harton, W.R. Hix, T. Horn, C.R. Howell, Y. Ilieva, B. Jacak, C. Keppel, O. Ketster, J. Klein, K. Kumar, K. Leach, D. Lee, S. Lescher, C.Y. Liu, J. Lopez, C. Lunardini, R. Milner, F. Nunes, D. Phillips, J. Piekarewicz, D. Pokanic, J. Qiu, S. Quaglioni, D. Radford, R. Reed, L. Ruan, M. Savage, C. Scarlett, B. Schenke, D.T. Takaki, D. Teaney, B. Van Devender, R. Vogt, N. Wall, F. Wietfeldt, J. Wilkerson, R. Wilson, L. Winslow, S. Yennello, X. Zheng, A new era of discovery: the 2023 long-range plan for nuclear science, 2023, https://doi.org/10.2172/2212868

[2] B.P. Abbott, R. Abbott, T.D. Abbott, F. Acernese, K. Ackley, C. Adams, T. Adams, P. Addesso, R.X. Adhikari, V.B. Adya, C. Affeldt, M. Afrough, B. Agarwal, M. Agathos, K. Agatsuma, N. Aggarwal, O.D. Aguiar, L. Aiello, A. Ain, P. Ajith, B. Allen, G. Allen, A. Allocca, P.A. Altin, A. Amato, A. Ananyeva, S.B. Anderson, W.G. Anderson, S.V. Angelova, S. Antier, S. Appert, K. Arai, M.C. Araya, J.S. Areeda, N. Arnaud, K.G. Arun, S. Ascenzi, G. Ashton, M. Ast, S.M. Aston, P. Astone, D.V. Atallah, P. Aufmuth, C. Aulbert, K. AultONeal, C. Austin, A. Avila-Alvarez, S. Babak, P. Bacon, M.K.M. Bader, S. Bae, M. Bailes, P.T. Baker, F. Baldaccini, G. Ballardin, S.W. Ballmer, S. Banagiri, J.C. Barayoga, S.E. Barclay, B.C. Barish, D. Barker, K. Barkett, F. Barone, B. Barr, L. Barsotti, M. Barsuglia, D. Barta, S.D. Barthelmy, J. Bartlett, I. Bartos, R. Bassiri, A. Basti, J.C. Batch, M. Bawaj, J.C. Bayley, M. Bazzan, B. Bécsy, C. Beer, M. Bejger, I. Belahcene, A.S. Bell, B.K. Berger, G. Bergmann, S. Bernuzzi, J.J. Bero, C.P.L. Berry, D. Bersanetti, A. Bertolini, J. Betzwieser, S. Bhagwat, R. Bhandare, I.A. Bilenko, G. Billingsley, C.R. Billman, J. Birch, R. Birney, O. Birnholtz, S. Biscans, S. Biscoveanu, A. Bisht, M. Bitossi, C. Biwer, M.A. Bizouard, J.K. Blackburn, J. Blackman, C.D. Blair, D.G. Blair, R.M. Blair, S. Bloemen, O. Bock, N. Bode, M. Boer, G. Bogaert, A. Bohe, F. Bondu, E. Bonilla, R. Bonnand, B.A. Boom, R. Bork, V. Boschi, S. Bose, K. Bossie, Y. Bouffanais, A. Bozzi, C. Bradaschia, P.R. Brady, M. Branchesi, J.E. Brau, T. Briant, A. Brillet, M. Brinkmann, V. Brisson, P. Brockill, J.E. Broida, A.F. Brooks, D.A. Brown, D.D. Brown, S. Brunett, C.C. Buchanan, A. Buikema, T. Bulik, H.J. Bulten, A. Buonanno, D. Buskulic, C. Buy, R.L. Byer, M. Cabero, L. Cadonati, G. Cagnoli, C. Cahillane, J. Calderón Bustillo, T.A. Callister, E. Calloni, J.B. Camp, M. Canepa, P. Canizares, K.C. Cannon, H. Cao, J. Cao, C.D. Capano, E. Capocasa, F. Carbognani, S. Caride, M.F. Carney, G. Carullo, J. Casanueva Diaz, C. Casentini, S. Caudill, M. Cavaglià, F. Cavalier, R. Cavalieri, G. Cella, C.B. Cepeda, P. Cerdá-Durán, G. Cerretani, E. Cesarini, S.J. Chamberlin, M. Chan, S. Chao, P. Charlton, E. Chase, E. Chassande-Mottin, D. Chatterjee, K. Chatziioannou, B.D. Cheeseboro, H.Y. Chen, X. Chen, Y. Chen, H.-P. Cheng, H. Chia, A. Chincarini, A. Chiummo, T. Chmiel, H.S. Cho, M. Cho, J.H. Chow, N. Christensen, Q. Chu, A.J.K. Chua, S. Chua, A.K.W. Chung, S. Chung, G. Ciani, R. Ciolfi, C.E. Cirelli, A. Cirone, F. Clara, J.A. Clark, P. Clearwater, F. Cleva, C. Cocchieri, E. Coccia, P.-F. Cohadon, D. Cohen, A. Colla, C.G. Collette, L.R. Cominsky, M. Constancio, L. Conti, S.J. Cooper, P. Corban, T.R. Corbitt, I. Cordero-Carrión, K.R. Corley, N. Cornish, A. Corsi, S. Cortese, C.A. Costa, M.W. Coughlin, S.B. Coughlin, J.-P. Coulon, S.T. Countryman, P. Couvares, P.B. Covas, E.E. Cowan, D.M. Coward, M.J. Cowart, D.C. Coyne, R. Coyne, J.D.E. Creighton, T.D. Creighton, J. Cripe, S.G. Crowder, T.J. Cullen, A. Cumming, L. Cunningham, E. Cuoco, T. Dal Canton, G. Dálya, S.L. Danilishin, S. D'Antonio, K. Danzmann, A. Dasgupta, C.F. Da Silva Costa, V. Dattilo, I. Dave, M. Davier, D. Davis, E.J. Daw, B. Day, S. De, D. DeBra, J. Degallaix, M. De Laurentis, S. Deléglise, W. Del Pozzo, N. Demos, T. Denker, T. Dent, R. De Pietri, V. Dergachev, R. De Rosa, R.T. DeRosa, C. De Rossi, R. DeSalvo, O. de Varona, J. Devenson, S. Dhurandhar, M.C. Díaz, T. Dietrich, L. Di Fiore, M. Di Giovanni, T. Di Girolamo, A. Di Lieto, S. Di Pace, I. Di Palma, F. Di Renzo, Z. doctor, V. Dolique, F. Donovan, K.L. Dooley, S. Doravari, I. Dorrington, R. Douglas, M. Dovale Álvarez, T.P. Downes, M. Drago, C. Dreissigacker, J.C. Driggers, Z. Du, M. Ducrot, R. Dudi, P. Dupej, S.E. Dwyer, T.B. Edo, M.C. Edwards, A. Effler, H.-B. Eggenstein, P. Ehrens, J. Eichholz, S.S. Eikenberry, R.A. Eisenstein, R.C. Essick, D. Estevez, Z.B. Etienne, T. Etzel, M. Evans, T.M. Evans, M. Factourovich, V. Fafone, H. Fair, S. Fairhurst, X. Fan, S. Farinon, B. Farr, W.M. Farr, E.J. Fauchon-Jones, M. Favata, M. Fays, C. Fee, H. Fehrmann, J. Feicht, M.M. Fejer,

A. Fernandez-Galiana, I. Ferrante, E.C. Ferreira, F. Ferrini, F. Fidecaro, D. Finstad, I. Fiori, D. Fiorucci, M. Fishbach, R.P. Fisher, M. Fitz-Axen, R. Flaminio, M. Fletcher, H. Fong, J.A. Font, P.W.F. Forsyth, S.S. Forsyth, J.-D. Fournier, S. Frasca, F. Frasconi, Z. Frei, A. Freise, R. Frey, V. Frey, E.M. Fries, P. Fritschel, V.V. Frolov, P. Fulda, M. Fyffe, H. Gabbard, B.U. Gadre, S.M. Gaebel, J.R. Gair, L. Gammaitoni, M.R. Ganija, S.G. Gaonkar, C. Garcia-Quiros, F. Garufi, B. Gateley, S. Gaudio, G. Gaur, V. Gayathri, N. Gehrels, G. Gemme, E. Genin, A. Gennai, D. George, J. George, L. Gergely, V. Germain, S. Ghonge, A. Ghosh, A. Ghosh, S. Ghosh, J.A. Giaime, K.D. Giardina, A. Giazotto, K. Gill, L. Glover, E. Goetz, R. Goetz, S. Gomes, B. Goncharov, G. González, J.M. Gonzalez Castro, A. Gopakumar, M.L. Gorodetsky, S.E. Gossan, M. Gosselin, R. Gouaty, A. Grado, C. Graef, M. Granata, A. Grant, S. Gras, C. Gray, G. Greco, A.C. Green, E.M. Gretarsson, P. Groot, H. Grote, S. Grunewald, P. Gruning, G.M. Guidi, X. Guo, A. Gupta, M.K. Gupta, K.E. Gushwa, E.K. Gustafson, R. Gustafson, O. Halim, B.R. Hall, E.D. Hall, E.Z. Hamilton, G. Hammond, M. Haney, M.M. Hanke, J. Hanks, C. Hanna, M.D. Hannam, O.A. Hannuksela, J. Hanson, T. Hardwick, J. Harms, G.M. Harry, I.W. Harry, M.J. Hart, C.-J. Haster, K. Haughian, J. Healy, A. Heidmann, M.C. Heintze, H. Heitmann, P. Hello, G. Hemming, M. Hendry, I.S. Heng, J. Hennig, A.W. Heptonstall, M. Heurs, S. Hild, T. Hinderer, W.C.G. Ho, D. Hoak, D. Hofman, K. Holt, D.E. Holz, P. Hopkins, C. Horst, J. Hough, E.A. Houston, E.J. Howell, A. Hreibi, Y.M. Hu, E.A. Huerta, D. Huet, B. Hughey, S. Husa, S.H. Huttner, T. Huynh-Dinh, N. Indik, R. Inta, G. Intini, H.N. Isa, J.-M. Isac, M. Isi, B.R. Iyer, K. Izumi, T. Jacqmin, K. Jani, P. Jaranowski, S. Jawahar, F. Jiménez-Forteza, W.W. Johnson, N.K. Johnson-McDaniel, D.I. Jones, R. Jones, R.J.G. Jonker, L. Ju, J. Junker, C.V. Kalaghatgi, V. Kalogera, B. Kamai, S. Kandhasamy, G. Kang, J.B. Kanner, S.J. Kapadia, S. Karki, K.S. Karvinen, M. Kasprzack, W. Kastaun, M. Katolik, E. Katsavounidis, W. Katzman, S. Kaufer, K. Kawabe, F. Kéfélian, D. Keitel, A.J. Kemball, R. Kennedy, C. Kent, J.S. Key, F.Y. Khalili, I. Khan, S. Khan, Z. Khan, E.A. Khazanov, N. Kijbunchoo, C. Kim, J.C. Kim, K. Kim, W. Kim, W.S. Kim, Y.-M. Kim, S.J. Kimbrell, E.J. King, P.J. King, M. Kinley-Hanlon, R. Kirchhoff, J.S. Kissel, L. Kleybolte, S. Klimenko, T.D. Knowles, P. Koch, S.M. Koehlenbeck, S. Koley, V. Kondrashov, A. Kontos, M. Korobko, W.Z. Korth, I. Kowalska, D.B. Kozak, C. Krämer, V. Kringel, B. Krishnan, A. Królak, G. Kuehn, P. Kumar, R. Kumar, S. Kumar, L. Kuo, A. Kutynia, S. Kwang, B.D. Lackey, K.H. Lai, M. Landry, R.N. Lang, J. Lange, B. Lantz, R.K. Lanza, S.L. Larson, A. Lartaux-Vollard, P.D. Lasky, M. Laxen, A. Lazzarini, C. Lazzaro, P. Leaci, S. Leavey, C.H. Lee, H.K. Lee, H.M. Lee, H.W. Lee, K. Lee, J. Lehmann, A. Lenon, E. Leon, M. Leonardi, N. Leroy, N. Letendre, Y. Levin, T.G.F. Li, S.D. Linker, T.B. Littenberg, J. Liu, X. Liu, R.K.L. Lo, N.A. Lockerbie, L.T. London, J.E. Lord, M. Lorenzini, V. Loriette, M. Lormand, G. Losurdo, J.D. Lough, C.O. Lousto, G. Lovelace, H. Lück, D. Lumaca, A.P. Lundgren, R. Lynch, Y. Ma, R. Macas, S. Macfoy, B. Machenschalk, M. MacInnis, D.M. Macleod, I. Magaña Hernandez, F. Magaña-Sandoval, L. Magaña Zertuche, R.M. Magee, E. Majorana, I. Maksimovic, N. Man, V. Mandic, V. Mangano, G.L. Mansell, M. Manske, M. Mantovani, F. Marchesoni, F. Marion, S. Márka, Z. Márka, C. Markakis, A.S. Markosyan, A. Markowitz, E. Maros, A. Marquina, P. Marsh, F. Martelli, L. Martellini, I.W. Martin, R.M. Martin, D.V. Martynov, J.N. Marx, K. Mason, E. Massera, A. Masserot, T.J. Massinger, M. Masso-Reid, S. Mastrogiovanni, A. Matas, F. Matichard, L. Matone, N. Mavalvala, N. Mazumder, R. McCarthy, D.E. McClelland, S. McCormick, L. McCuller, S.C. McGuire, G. McIntyre, J. McIver, D.J. McManus, L. McNeill, T. McRae, S.T. McWilliams, D. Meacher, G.D. Meadors, M. Mehmet, J. Meidam, E. Mejuto-Villa, A. Melatos, G. Mendell, R.A. Mercer, E.L. Merilh, M. Merzougui, S. Meshkov, C. Messenger, C. Messick, R. Metzdorff, P.M. Meyers, H. Miao, C. Michel, H. Middleton, E.E. Mikhailov, L. Milano, A.L. Miller, B.B. Miller, J. Miller, M. Millhouse, M.C. Milovich-Goff, O. Minazzoli, Y. Minenkov, J. Ming, C. Mishra, S. Mitra, V.P. Mitrofanov, G. Mitselmakher, R. Mittleman, D. Moffa, A. Moggi, K. Mogushi, M. Mohan, S.R.P. Mohapatra, I. Molina, M. Montani, C.J. Moore, D. Moraru, G. Moreno, S. Morisaki, S.R. Morriss, B. Mours, C.M. Mow-Lowry, G. Mueller, A.W. Muir, A. Mukherjee, D. Mukherjee, S. Mukherjee, N. Mukund, A. Mullavey, J. Munch, E.A. Muñiz, M. Muratore, P.G. Murray, A. Nagar, K. Napier, I. Nardecchia, L. Naticchioni, R.K. Nayak, J. Neilson, G. Nelemans, T.J.N. Nelson, M. Nery, A. Neunzert, L. Nevin, J.M. Newport, G. Newton, K.K.Y. Ng, P. Nguyen, T.T. Nguyen, D. Nichols, A.B. Nielsen, S. Nissanke, A. Nitz, A. Noack, F. Nocera, D. Nolting, C. North, L.K. Nuttall, J. Oberling, G.D. O'Dea, G.H. Ogin, J.J. Oh, S.H. Oh, F. Ohme, M.A. Okada, M. Oliver, P. Oppermann, R.J. Oram, B. O'Reilly, R. Ormiston, L.F. Ortega, R. O'Shaughnessy, S. Ossokine, D.J. Ottaway, H. Overmier, B.J. Owen, A.E. Pace, J. Page, M.A. Page, A. Pai, S.A. Pai, J.R. Palamos, O. Palashov, C. Palomba, A. Pal-Singh, H. Pan, H.-W. Pan, B. Pang, P.T.H. Pang, C. Pankow, F. Pannarale, B.C. Pant, F. Paoletti, A. Paoli, M.A. Papa, A. Parida, W. Parker, D. Pascucci, A. Pasqualetti, R. Passaquieti, D. Passuello, M. Patil, B. Patricelli, B.L. Pearlstone, M. Pedraza, R. Pedurand, L. Pekowsky, A. Pele, S. Penn, C.J. Perez, A. Perreca, L.M. Perri, H.P. Pfeiffer, M. Phelps, O.J. Piccinni, M. Pichot, F. Piergiovanni, V. Pierro, G. Pillant, L. Pinard, I.M. Pinto, M. Pirello, M. Pitkin, M. Poe, R. Poggiani, P. Popolizio, E.K. Porter, A. Post, J. Powell, J. Prasad, J.W.W. Pratt, G. Pratten, V. Predoi, T. Prestegard, M. Prijatelj, M. Principe, S. Privitera, R. Prix, G.A. Prodi, L.G. Prokhorov, O. Puncken, M. Punturo, P. Puppo, M. Pürrer, H. Qi, V. Quetschke, E.A. Quintero, R. Quitzow-James, F.J. Raab, D.S. Rabeling, H. Radkins, P. Raffai, S. Raja, C. Rajan, B. Rajbhandari, M. Rakhmanov, K.E. Ramirez, A. Ramos-Buades, P. Rapagnani, V. Raymond, M. Razzano, J. Read, T. Regimbau, L. Rei, S. Reid, D.H. Reitze, W. Ren, S.D. Reyes, F. Ricci, P.M. Ricker, S. Rieger, K. Riles, M. Rizzo, N.A. Robertson, R. Robie, F. Robinet, A. Rocchi, L. Rolland, J.G. Rollins, V.J. Roma, J.D. Romano, R. Romano, C.L. Romel, J.H. Romie, D. Rosińska, M.P. Ross, S. Rowan, A. Rüdiger, P. Ruggi, G. Rutins, K. Ryan, S. Sachdev, T. Sadecki, L. Sadeghian, M. Sakellariadou, L. Salconi, M. Saleem, F. Salemi, A. Samajdar, L. Sammut, L.M. Sampson, E.J. Sanchez, L.E. Sanchez, N. Sanchis-Gual, V. Sandberg, J.R. Sanders, B. Sassolas, B.S. Sathyaprakash, P.R. Saulson, O. Sauter, R.L. Savage, A. Sawadsky, P. Schale, M. Scheel, J. Scheuer, J. Schmidt, P. Schmidt, R. Schnabel, R.M.S. Schofield, A. Schönbeck, E. Schreiber, D. Schuette, B.W. Schulte, B.F. Schutz, S.G. Schwalbe, J. Scott, S.M. Scott, E. Seidel, D. Sellers, A.S. Sengupta, D. Sentenac, V. Sequino, A. Sergeev, D.A. Shaddock, T.J. Shaffer, A.A. Shah, M.S. Shahriar, M.B. Shaner, L. Shao, B. Shapiro, P. Shawhan, A. Sheperd, D.H. Shoemaker, D.M. Shoemaker, K. Siellez, X. Siemens, M. Sieniawska, D. Sigg, A.D. Silva, L.P. Singer, A. Singh, A. Singhal, A.M. Sintes, B.J.J. Slagmolen, B. Smith, J.R. Smith, R.J.E. Smith, S. Somala, E.J. Son, J.A. Sonnenberg, B. Sorazu, F. Sorrentino, T. Souradeep, A.P. Spencer, A.K. Srivastava, K. Staats, A. Staley, M. Steinke, J. Steinlechner, S. Steinlechner, D. Steinmeyer, S.P. Stevenson, R. Stone, D.J. Stops, K.A. Strain, G. Stratta, S.E. Strigin, A. Strunk, R. Sturani, A.L. Stuver, T.Z. Summerscales, L. Sun, S. Sunil, J. Suresh, P.J. Sutton, B.L. Swinkels, M.J. Szczepańczyk, M. Tacca, S.C. Tait, C. Talbot, D. Talukder, D.B. Tanner, M. Tápai, A. Taracchini, J.D. Tasson, J.A. Taylor, R. Taylor, S.V. Tewari, T. Theeg, F. Thies, E.G. Thomas, M. Thomas, P. Thomas, K.A. Thorne, K.S. Thorne, E. Thrane, S. Tiwari, V. Tiwari, K.V. Tokmakov, K. Toland, M. Tonelli, Z. Tornasi, A. Torres-Forné, C.I. Torrie, D. Töyrä, F. Travasso, G. Traylor, J. Trinastic, M.C. Tringali, L. Trozzo, K.W. Tsang, M. Tse, R. Tso, L. Tsukada, D. Tsuna, D. Tuyenbayev, K. Ueno, D. Ugolini, C.S. Unnikrishnan, A.L. Urban, S.A. Usman, H. Vahlbruch, G. Vajente, G. Valdes, M. Vallisneri, N. van Bakel, M. van Beuzekom, J.F.J. van den Brand, C. Van Den Broeck, D.C. Vander-Hyde, L. van der Schaaf, J.V. van Heijningen, A.A. van Veggel, M. Vardaro, V. Varma, S. Vass, M. Vasúth, A. Vecchio, G. Vedovato, J. Veitch, P.J. Veitch, K. Venkateswara, G. Venugopalan, D. Verkindt, F. Vetrano, A. Viceré, A.D. Viets, S. Vinciguerra, D.J. Vine, J.-Y. Vinet, S. Vitale, T. Vo, H. Vocca, C. Vorvick, S.P. Vyatchanin, A.R. Wade, L.E. Wade, M. Wade, R. Walet, M. Walker, L. Wallace, S. Walsh, G. Wang, H. Wang, J.Z. Wang, W.H. Wang, Y.F. Wang, R.L. Ward, J. Warner, M. Was, J. Watchi, B. Weaver, L.-W. Wei, M. Weinert, A.J. Weinstein, R. Weiss, L. Wen, E.K. Wessel, P. Weßels, J. Westerweck, T. Westphal, K. Wette, J.T. Whelan, S.E. Whitcomb, B.F. Whiting, C. Whittle, D. Wilken, D. Williams, R.D. Williams, A.R. Williamson, J.L. Willis, B. Willke, M.H. Wimmer, W. Winkler, C.C. Wipf, H. Wittel, G. Woan, J. Woehler, J. Wofford, K.W.K. Wong, J. Worden, J.L. Wright, D.S. Wu, D.M. Wysocki, S. Xiao, H. Yamamoto, C.C. Yancey, L. Yang, M.J. Yap, M. Yazback, H. Yu, H. Yu, M. Yvert, A. Zadrożny, M. Zanolin, T. Zelenova, J.-P. Zendri, M. Zevin, L. Zhang, M. Zhang, T. Zhang, Y.-H. Zhang, C. Zhao, M. Zhou, Z. Zhou, S.J. Zhu, X.J. Zhu, A.B. Zimmerman, M.E. Zucker, J. Zweizig, V. Collaboration, LIGO Scientific and Collaboration, GW170817: Observation of gravitational waves from a binary neutron star inspiral, Phys. Rev. Lett. 119 (16) (2017) 161101. https://doi.org/10.1103/PhysRevLett.119.161101

[3] B.P. Abbott, R. Abbott, T.D. Abbott, F. Acernese, K. Ackley, C. Adams, T. Adams, P. Addesso, R.X. Adhikari, V.B. Adya, C. Affeldt, B. Agarwal, M. Agathos, K. Agatsuma, N. Aggarwal, O.D. Aguiar, L. Aiello, A. Ain, P. Ajith, B. Allen, G. Allen, A. Allocca, M.A. Aloy, P.A. Altin, A. Amato, A. Ananyeva, S.B. Anderson, W.G. Anderson, S.V. Angelova, S. Antier, S. Appert, K. Arai, M.C. Araya, J.S. Areeda, M. Arène, N. Arnaud, K.G. Arun, S. Ascenzi, G. Ashton, M. Ast, S.M. Aston, P. Astone, D.V. Atallah, F. Aubin, P. Aufmuth, C. Aulbert, K. AultONeal, C. Austin, A. Avila-Alvarez, S. Babak, P. Bacon, F. Badaracco, M.K.M. Bader, S. Bae, P.T. Baker, F. Baldaccini, G. Ballardin, S.W. Ballmer, S. Banagiri, J.C. Barayoga, S.E. Barclay, B.C. Barish, D. Barker, K. Barkett, S. Barnum, F. Barone, B. Barr, L. Barsotti, M. Barsuglia, D. Barta, J. Bartlett, I. Bartos, R. Bassiri, A. Basti, J.C. Batch, M. Bawaj, J.C. Bayley, M. Bazzan, B. Bécsy, C. Beer, M. Bejger, I. Belahcene, A.S. Bell, D. Beniwal, M. Bensch, B.K. Berger, G. Bergmann, S. Bernuzzi, J.J. Bero, C.P.L. Berry, D. Bersanetti, A. Bertolini, J. Betzwieser, R. Bhandare, I.A. Bilenko, S.A. Bilgili, G. Billingsley, C.R. Billman, J. Birch, R. Birney, O. Birnholtz, S. Biscans, S. Biscoveanu, A. Bisht, M. Bitossi, M.A. Bizouard, J.K. Blackburn, J. Blackman, C.D. Blair, D.G. Blair, R.M. Blair, S. Bloemen, O. Bock, N. Bode, M. Boer, Y. Boetzel, G. Bogaert, A. Bohe, F. Bondu, E. Bonilla, R. Bonnand, P. Booker, B.A. Boom, C.D. Booth, R. Bork, V. Boschi, S. Bose, K. Bossie, V. Bossilkov, J. Bosveld, Y. Bouffanais, A. Bozzi, C. Bradaschia, P.R. Brady, A. Bramley, M. Branchesi, J.E. Brau, T. Briant, F. Brighenti, A. Brillet, M. Brinkmann, V. Brisson, P. Brockill, A.F. Brooks, D.D. Brown, S. Brunett, C.C. Buchanan, A. Buikema, T. Bulik, H.J. Bulten, A. Buonanno, D. Buskulic, C. Buy, R.L. Byer, M. Cabero, L. Cadonati, G. Cagnoli, C. Cahillane, J. Calderón Bustillo, T.A. Callister, E. Calloni, J.B. Camp, M. Canepa, P. Canizares, K.C. Cannon, H. Cao, J. Cao, C.D. Capano, E. Capocasa, F. Carbognani, S. Caride, M.F. Carney, G. Carullo, J. Casanueva Diaz, C. Casentini, S. Caudill, M. Cavaglià, F. Cavalier, R. Cavalieri, G. Cella, C.B. Cepeda, P. Cerdá-Durán, G. Cerretani, E. Cesarini, O. Chaibi, S.J. Chamberlin, M. Chan, S. Chao, P. Charlton, E. Chase, E. Chassande-Mottin, D. Chatterjee, K. Chatziioannou, B.D. Cheeseboro, H.Y. Chen, X. Chen, Y. Chen, H.-P. Cheng, H.Y. Chia, A. Chincarini, A. Chiummo, T. Chmiel, H.S. Cho, M. Cho, J.H. Chow, N. Christensen, Q. Chu, A.J.K. Chua, S. Chua, K.W. Chung, S. Chung, G. Ciani, A.A. Ciobanu, R. Ciolfi, F. Cipriano, C.E. Cirelli, A. Cirone, F. Clara, J.A. Clark, P. Clearwater, F. Cleva, C. Cocchieri, E. Coccia, P.-F. Cohadon, D. Cohen, A. Colla, C.G. Collette, C. Collins, L.R. Cominsky, M. Constancio, L. Conti, S.J. Cooper, P. Corban, T.R. Corbitt, I. Cordero-Carrión, K.R. Corley, N. Cornish, A. Corsi, S. Cortese, C.A. Costa, R. Cotesta, M.W. Coughlin, S.B. Coughlin, J.-P. Coulon, S.T. Countryman, P. Couvares, P.B. Covas, E.E. Cowan, D.M. Coward, M.J. Cowart, D.C. Coyne, R. Coyne, J.D.E. Creighton, T.D. Creighton, J. Cripe, S.G. Crowder, T.J. Cullen, A. Cumming, L. Cunningham, E. Cuoco, T.D. Canton, G. Dálya, S.L. Danilishin, S. D'Antonio, K. Danzmann, A. Dasgupta, C.F. Da Silva Costa, V. Dattilo, I. Dave, M. Davier, D. Davis, E.J. Daw, B. Day, D. DeBra, M. Deenadayalan, J. Degallaix, M. De Laurentis, S. Deléglise, W. Del Pozzo, N. Demos, T. Denker, T. Dent, R. De Pietri, J. Derby, V. Dergachev, R. De Rosa, C. De Rossi, R. DeSalvo, O. de Varona, S. Dhurandhar, M.C. Díaz, T. Dietrich, L. Di Fiore, M. Di Giovanni, T. Di Girolamo, A. Di Lieto, B. Ding, S. Di Pace, I. Di Palma, F. Di Renzo, A. Dmitriev, Z. doctor, V. Dolique, F. Donovan, K.L. Dooley, S. Doravari, I. Dorrington, M. Dovale Álvarez, T.P. Downes, M. Drago, C. Dreissigacker, J.C. Driggers, Z. Du, P. Dupej, S.E. Dwyer, P.J. Easter, T.B. Edo, M.C. Edwards, A. Effler, H.-B. Eggenstein, P. Ehrens, J. Eichholz, S.S. Eikenberry, M. Eisenmann, R.A. Eisenstein, R.C. Essick, H. Estelles, D. Estevez, Z.B. Etienne, T. Etzel, M. Evans, T.M. Evans, V. Fafone, H. Fair, S. Fairhurst, X. Fan, S. Farinon, B. Farr, W.M. Farr, E.J. Fauchon-Jones, M. Favata, M. Fays, C. Fee, H. Fehrmann, J. Feicht, M.M. Fejer, F. Feng, A. Fernandez-Galiana, I. Ferrante, E.C. Ferreira, F. Ferrini, F. Fidecaro, I. Fiori, D. Fiorucci, M. Fishbach, R.P. Fisher, J.M.

Fishner, M. Fitz-Axen, R. Flaminio, M. Fletcher, H. Fong, J.A. Font, P.W.F. Forsyth, S.S. Forsyth, J.-D. Fournier, S. Frasca, F. Frasconi, Z. Frei, A. Freise, R. Frey, V. Frey, P. Fritschel, V.V. Frolov, P. Fulda, M. Fyffe, H.A. Gabbard, B.U. Gadre, S.M. Gaebel, J.R. Gair, L. Gammaitoni, M.R. Ganija, S.G. Gaonkar, A. Garcia, C. García-Quirós, F. Garufi, B. Gateley, S. Gaudio, G. Gaur, V. Gayathri, G. Gemme, E. Genin, A. Gennai, D. George, J. George, L. Gergely, V. Germain, S. Ghonge, A. Ghosh, A. Ghosh, S. Ghosh, B. Giacomazzo, J.A. Giaime, K.D. Giardina, A. Giazotto, K. Gill, G. Giordano, L. Glover, E. Goetz, R. Goetz, B. Goncharov, G. González, J.M. Gonzalez Castro, A. Gopakumar, M.L. Gorodetsky, S.E. Gossan, M. Gosselin, R. Gouaty, A. Grado, C. Graef, M. Granata, A. Grant, S. Gras, C. Gray, G. Greco, A.C. Green, R. Green, E.M. Gretarsson, P. Groot, H. Grote, S. Grunewald, P. Gruning, G.M. Guidi, H.K. Gulati, X. Guo, A. Gupta, M.K. Gupta, K.E. Gushwa, E.K. Gustafson, R. Gustafson, O. Halim, B.R. Hall, E.D. Hall, E.Z. Hamilton, H.F. Hamilton, G. Hammond, M. Haney, M.M. Hanke, J. Hanks, C. Hanna, M.D. Hannam, O.A. Hannuksela, J. Hanson, T. Hardwick, J. Harms, G.M. Harry, I.W. Harry, M.J. Hart, C.-J. Haster, K. Haughian, J. Healy, A. Heidmann, M.C. Heintze, H. Heitmann, P. Hello, G. Hemming, M. Hendry, I.S. Heng, J. Hennig, A.W. Heptonstall, F.J. Hernandez, M. Heurs, S. Hild, T. Hinderer, W.C.G. Ho, D. Hoak, S. Hochheim, D. Hofman, N.A. Holland, K. Holt, D.E. Holz, P. Hopkins, C. Horst, J. Hough, E.A. Houston, E.J. Howell, A. Hreibi, E.A. Huerta, D. Huet, B. Hughey, M. Hulko, S. Husa, S.H. Huttner, T. Huynh-Dinh, A. Iess, N. Indik, C. Ingram, R. Inta, G. Intini, B.S. Irwin, H.N. Isa, J.-M. Isac, M. Isi, B.R. Iyer, K. Izumi, T. Jacqmin, K. Jani, P. Jaranowski, D.S. Johnson, W.W. Johnson, D.I. Jones, R. Jones, R.J.G. Jonker, L. Ju, J. Junker, C.V. Kalaghatgi, V. Kalogera, B. Kamai, S. Kandhasamy, G. Kang, J.B. Kanner, S.J. Kapadia, S. Karki, K.S. Karvinen, M. Kasprzack, M. Katolik, S. Katsanevas, E. Katsavounidis, W. Katzman, S. Kaufer, K. Kawabe, N.V. Keerthana, F. Kéfélian, D. Keitel, A.J. Kemball, R. Kennedy, J.S. Key, F.Y. Khalili, B. Khamesra, H. Khan, I. Khan, S. Khan, Z. Khan, E.A. Khazanov, N. Kijbunchoo, C. Kim, J.C. Kim, K. Kim, W. Kim, W.S. Kim, Y.-M. Kim, E.J. King, P.J. King, M. Kinley-Hanlon, R. Kirchhoff, J.S. Kissel, L. Kleybolte, S. Klimenko, T.D. Knowles, P. Koch, S.M. Koehlenbeck, S. Koley, V. Kondrashov, A. Kontos, M. Korobko, W.Z. Korth, I. Kowalska, D.B. Kozak, C. Krämer, V. Kringel, B. Krishnan, A. Królak, G. Kuehn, P. Kumar, R. Kumar, S. Kumar, L. Kuo, A. Kutynia, S. Kwang, B.D. Lackey, K.H. Lai, M. Landry, P. Landry, R.N. Lang, J. Lange, B. Lantz, R.K. Lanza, A. Lartaux-Vollard, P.D. Lasky, M. Laxen, A. Lazzarini, C. Lazzaro, P. Leaci, S. Leavey, C.H. Lee, H.K. Lee, H.M. Lee, H.W. Lee, K. Lee, J. Lehmann, A. Lenon, M. Leonardi, N. Leroy, N. Letendre, Y. Levin, J. Li, T.G.F. Li, X. Li, S.D. Linker, T.B. Littenberg, J. Liu, X. Liu, R.K.L. Lo, N.A. Lockerbie, L.T. London, A. Longo, M. Lorenzini, V. Loriette, M. Lormand, G. Losurdo, J.D. Lough, C.O. Lousto, G. Lovelace, H. Lück, D. Lumaca, A.P. Lundgren, R. Lynch, Y. Ma, R. Macas, S. Macfoy, B. Machenschalk, M. MacInnis, D.M. Macleod, I. Magaña Hernandez, F. Magaña-Sandoval, L. Magaña Zertuche, R.M. Magee, E. Majorana, I. Maksimovic, N. Man, V. Mandic, V. Mangano, G.L. Mansell, M. Manske, M. Mantovani, F. Marchesoni, F. Marion, S. Márka, Z. Márka, C. Markakis, A.S. Markosyan, A. Markowitz, E. Maros, A. Marquina, F. Martelli, L. Martellini, I.W. Martin, R.M. Martin, D.V. Martynov, K. Mason, E. Massera, A. Masserot, T.J. Massinger, M. Masso-Reid, S. Mastrogiovanni, A. Matas, F. Matichard, L. Matone, N. Mavalvala, N. Mazumder, J.J. McCann, R. McCarthy, D.E. McClelland, S. McCormick, L. McCuller, S.C. McGuire, J. McIver, D.J. McManus, T. McRae, S.T. McWilliams, D. Meacher, G.D. Meadors, M. Mehmet, J. Meidam, E. Mejuto-Villa, A. Melatos, G. Mendell, D. Mendoza-Gandara, R.A. Mercer, L. Mereni, E.L. Merilh, M. Merzougui, S. Meshkov, C. Messenger, C. Messick, R. Metzdorff, P.M. Meyers, H. Miao, C. Michel, H. Middleton, E.E. Mikhailov, L. Milano, A.L. Miller, A. Miller, B.B. Miller, J. Miller, M. Millhouse, J. Mills, M.C. Milovich-Goff, O. Minazzoli, Y. Minenkov, J. Ming, C. Mishra, S. Mitra, V.P. Mitrofanov, G. Mitselmakher, R. Mittleman, D. Moffa, K. Mogushi, M. Mohan, S.R.P. Mohapatra, M. Montani, C.J. Moore, D. Moraru, G. Moreno, S. Morisaki, B. Mours, C.M. Mow-Lowry, G. Mueller, A.W. Muir, A. Mukherjee, D. Mukherjee, S. Mukherjee, N. Mukund, A. Mullavey, J. Munch, E.A. Muñiz, M. Muratore, P.G. Murray, A. Nagar, K. Napier, I. Nardecchia, L. Naticchioni, R.K. Nayak, J. Neilson, G. Nelemans, T.J.N. Nelson, M. Nery, A. Neunzert, L. Nevin, J.M. Newport, K.Y. Ng, S. Ng, P. Nguyen, T.T. Nguyen, D. Nichols, A.B. Nielsen, S. Nissanke, A. Nitz, F. Nocera, D. Nolting, C. North, L.K. Nuttall, M. Obergaulinger, J. Oberling, B.D. O'Brien, G.D. O'Dea, G.H. Ogin, J.J. Oh, S.H. Oh, F. Ohme, H. Ohta, M.A. Okada, M. Oliver, P. Oppermann, R.J. Oram, B. O'Reilly, R. Ormiston, L.F. Ortega, R. O'Shaughnessy, S. Ossokine, D.J. Ottaway, H. Overmier, B.J. Owen, A.E. Pace, G. Pagano, J. Page, M.A. Page, A. Pai, S.A. Pai, J.R. Palamos, O. Palashov, C. Palomba, A. Pal-Singh, H. Pan, H.-W. Pan, B. Pang, P.T.H. Pang, C. Pankow, F. Pannarale, B.C. Pant, F. Paoletti, A. Paoli, M.A. Papa, A. Parida, W. Parker, D. Pascucci, A. Pasqualetti, R. Passaquieti, D. Passuello, M. Patil, B. Patricelli, B.L. Pearlstone, C. Pedersen, M. Pedraza, R. Pedurand, L. Pekowsky, A. Pele, S. Penn, A. Perego, C.J. Perez, A. Perreca, L.M. Perri, H.P. Pfeiffer, M. Phelps, K.S. Phukon, O.J. Piccinni, M. Pichot, F. Piergiovanni, V. Pierro, G. Pillant, L. Pinard, I.M. Pinto, M. Pirello, M. Pitkin, R. Poggiani, P. Popolizio, E.K. Porter, L. Possenti, A. Post, J. Powell, J. Prasad, J.W.W. Pratt, G. Pratten, V. Predoi, T. Prestegard, M. Principe, S. Privitera, G.A. Prodi, L.G. Prokhorov, O. Puncken, M. Punturo, P. Puppo, M. Pürrer, H. Qi, V. Quetschke, E.A. Quintero, R. Quitzow-James, F.J. Raab, D.S. Rabeling, H. Radkins, P. Raffai, S. Raja, C. Rajan, B. Rajbhandari, M. Rakhmanov, K.E. Ramirez, A. Ramos-Buades, J. Rana, P. Rapagnani, V. Raymond, M. Razzano, J. Read, T. Regimbau, L. Rei, S. Reid, D.H. Reitze, W. Ren, F. Ricci, P.M. Ricker, G.M. Riemenschneider, K. Riles, M. Rizzo, N.A. Robertson, R. Robie, F. Robinet, T. Robson, A. Rocchi, L. Rolland, J.G. Rollins, V.J. Roma, R. Romano, C.L. Romel, J.H. Romie, D. Rosińska, M.P. Ross, S. Rowan, A. Rüdiger, P. Ruggi, G. Rutins, K. Ryan, S. Sachdev, T. Sadecki, M. Sakellariadou, L. Salconi, M. Saleem, F. Salemi, A. Samajdar, L. Sammut, L.M. Sampson, E.J. Sanchez, L.E. Sanchez, N. Sanchis-Gual, V. Sandberg, J.R. Sanders, N. Sarin, B. Sassolas, B.S. Sathyaprakash, P.R. Saulson, O. Sauter, R.L. Savage, A. Sawadsky, P. Schale, M. Scheel, J. Scheuer, P. Schmidt, R. Schnabel, R.M.S. Schofield, A. Schönbeck, E. Schreiber, D. Schuette, B.W. Schulte, B.F. Schutz, S.G. Schwalbe, J. Scott, S.M. Scott, E. Seidel, D. Sellers, A.S. Sengupta, D. Sentenac, V. Sequino, A. Sergeev, Y. Setyawati, D.A. Shaddock, T.J. Shaffer, A.A. Shah, M.S. Shahriar, M.B. Shaner, L. Shao, B. Shapiro, P. Shawhan, H. Shen, D.H. Shoemaker, D.M. Shoemaker, K. Siellez, X. Siemens, M. Sieniawska, D. Sigg, A.D. Silva, L.P. Singer, A. Singh, A. Singhal, A.M. Sintes, B.J.J. Slagmolen, T.J. Slaven-Blair, B. Smith, J.R. Smith, R.J.E. Smith, S. Somala, E.J. Son, B. Sorazu, F. Sorrentino, T. Souradeep, A.P. Spencer, A.K. Srivastava, K. Staats, M. Steinke, J. Steinlechner, S. Steinlechner, D. Steinmeyer, B. Steltner, S.P. Stevenson, D. Stocks, R. Stone, D.J. Stops, K.A. Strain, G. Stratta, S.E. Strigin, A. Strunk, R. Sturani, A.L. Stuver, T.Z. Summerscales, L. Sun, S. Sunil, J. Suresh, P.J. Sutton, B.L. Swinkels, M.J. Szczepańczyk, M. Tacca, S.C. Tait, C. Talbot, D. Talukder, D.B. Tanner, M. Tápai, A. Taracchini, J.D. Tasson, J.A. Taylor, R. Taylor, S.V. Tewari, T. Theeg, F. Thies, E.G. Thomas, M. Thomas, P. Thomas, K.A. Thorne, E. Thrane, S. Tiwari, V. Tiwari, K.V. Tokmakov, K. Toland, M. Tonelli, Z. Tornasi, A. Torres-Forné, C.I. Torrie, D. Töyrä, F. Travasso, G. Traylor, J. Trinastic, M.C. Tringali, A. Trovato, L. Trozzo, K.W. Tsang, M. Tse, R. Tso, D. Tsuna, L. Tsukada, D. Tuyenbayev, K. Ueno, D. Ugolini, A.L. Urban, S.A. Usman, H. Vahlbruch, G. Vajente, G. Valdes, N. van Bakel, M. van Beuzekom, J.F.J. van den Brand, C. Van Den Broeck, D.C. Vander-Hyde, L. van der Schaaf, J.V. van Heijningen, A.A. van Veggel, M. Vardaro, V. Varma, S. Vass, M. Vasúth, A. Vecchio, G. Vedovato, J. Veitch, P.J. Veitch, K. Venkateswara, G. Venugopalan, D. Verkindt, F. Vetrano, A. Viceré, A.D. Viets, S. Vinciguerra, D.J. Vine, J.-Y. Vinet, S. Vitale, T. Vo, H. Vocca, C. Vorvick, S.P. Vyatchanin, A.R. Wade, L.E. Wade, M. Wade, R. Walet, M. Walker, L. Wallace, S. Walsh, G. Wang, H. Wang, J.Z. Wang, W.H. Wang, Y.F. Wang, R.L. Ward, J. Warner, M. Was, J. Watchi, B. Weaver, L.-W. Wei, M. Weinert, A.J. Weinstein, R. Weiss, F. Wellmann, L. Wen, E.K. Wessel, P. Weßels, J. Westerweck, K. Wette, J.T. Whelan, B.F. Whiting, C. Whittle, D. Wilken, D. Williams, R.D. Williams, A.R. Williamson, J.L. Willis, B. Willke, M.H. Wimmer, W. Winkler, C.C. Wipf, H. Wittel, G. Woan, J. Woehler, J.K. Wofford, W.K. Wong, J. Worden, J.L. Wright, D.S. Wu, D.M. Wysocki, S. Xiao, W. Yam, H. Yamamoto, C.C. Yancey, L. Yang, M.J. Yap, M. Yazback, H. Yu, H. Yu, M. Yvert, A. Zadrożny, M. Zanolin, T. Zelenova, J.-P. Zendri, M. Zevin, J. Zhang, L. Zhang, M. Zhang, T. Zhang, Y.-H. Zhang, C. Zhao, M. Zhou, Z. Zhou, S.J. Zhu, X.J. Zhu, A.B. Zimmerman, Y. Zlochower, M.E. Zucker, J. Zweizig, t.V. Collaboration, LIGO Scientific and Collaboration, GW170817: measurements of neutron star radii and equation of state, Phys. Rev. Lett. 121 (16) (2018) 161101. https://doi.org/10.1103/PhysRevLett.121.161101

[4] B.P. Abbott, R. Abbott, T.D. Abbott, S. Abraham, F. Acernese, K. Ackley, C. Adams, R.X. Adhikari, V.B. Adya, C. Affeldt, M. Agathos, K. Agatsuma, N. Aggarwal, O.D. Aguiar, L. Aiello, A. Ain, P. Ajith, G. Allen, A. Allocca, M.A. Aloy, P.A. Altin, A. Amato, S. Anand, A. Ananyeva, S.B. Anderson, W.G. Anderson, S.V. Angelova, S. Antier, S. Appert, K. Arai, M.C. Araya, J.S. Areeda, M. Arène, N. Arnaud, GW190425: observation of a compact binary coalescence with total mass $\sim 3.4\,M_{\odot}$, ApJL 892 (1) (2020) L3. arXiv:2001.01761https://doi.org/10.3847/2041-8213/ab75f5

[5] K.C. Gendreau, Z. Arzoumanian, T. Okajima, The neutron star interior composition explorer (NICER): an explorer mission of opportunity for soft x-ray timing spectroscopy, in: T. Takahashi, S.S. Murray, J.-W.A. den Herder (Eds.), Space Telescopes and Instrumentation 2012: ultraviolet to Gamma Ray, SPIE, 2012. https://doi.org/10.1117/12.926396

[6] S. Huth, P.T.H. Pang, I. Tews, T. Dietrich, A. Le Fèvre, A. Schwenk, W. Trautmann, K. Agarwal, M. Bulla, M.W. Coughlin, C. Van Den Broeck, Constraining neutron-star matter with microscopic and macroscopic collisions, Nature 606 (7913) (2022) 276–280. https://doi.org/10.1038/s41586-022-04750-w

[7] C.Y. Tsang, M.B. Tsang, W.G. Lynch, R. Kumar, C.J. Horowitz, Determination of the equation of state from nuclear experiments and neutron star observations, Nat. Astron. 8 (3) (2024) 328–336. https://doi.org/10.1038/s41550-023-02161-z

[8] C.Y. Tsang, M. Kurata-Nishimura, M.B. Tsang, W.G. Lynch, Y.X. Zhang, J. Barney, J. Estee, G. Jhang, R. Wang, M. Kaneko, J.W. Lee, T. Isobe, T. Murakami, D.S. Ahn, L. Atar, T. Aumann, H. Baba, K. Boretzky, J. Brzychczyk, G. Cerizza, N. Chiga, N. Fukuda, I. Gasparic, B. Hong, A. Horvat, K. Ieki, N. Inabe, Y.J. Kim, T. Kobayashi, Y. Kondo, P. Lasko, H.S. Lee, Y. Leifels, J. Łukasik, J. Manfredi, A.B. McIntosh, P. Morfouace, T. Nakamura, N. Nakatsuka, S. Nishimura, H. Otsu, P. Pawłowski, K. Pelczar, D. Rossi, H. Sakurai, C. Santamaria, H. Sato, H. Scheit, R. Shane, Y. Shimizu, H. Simon, A. Snoch, A. Sochocka, T. Sumikama, H. Suzuki, D. Suzuki, H. Takeda, S. Tangwancharoen, H. Törnqvist, Y. Togano, Z.G. Xiao, S.J. Yennello, Y. Zhang, Constraining nucleon effective masses with flow and stopping observables from the SπRIT experiment, Phys. Lett. B 853 (138661) (2024) 138661. https://doi.org/10.1016/j.physletb.2024.138661

[9] M.B. Tsang, W.G. Lynch, P. Danielewicz, C.Y. Tsang, Symmetry energy constraints from GW170817 and laboratory experiments, Phys. Lett. B 795 (2019) 533–536. https://doi.org/10.1016/j.physletb.2019.06.059

[10] H. Sakurai, RI Beam factory project at RIKEN, Nucl. Phys. A 805 (1) (2008) 526c–532c. https://doi.org/10.1016/j.nuclphysa.2008.02.291

[11] H.L. Crawford, V. Tripathi, J.M. Allmond, B.P. Crider, R. Grzywacz, S.N. Liddick, A. Andalib, E. Argo, C. Benetti, S. Bhattacharya, C.M. Campbell, M.P. Carpenter, J. Chan, A. Chester, J. Christie, B.R. Clark, I. Cox, A.A. Doetsch, J. Dopfer, J.G. Duarte, P. Fallon, A. Frotscher, T. Gaballah, T.J. Gray, J.T. Harke, J. Heideman, H. Heugen, R. Jain, T.T. King, N. Kitamura, K. Kolos, F.G. Kondev, A. Laminack, B. Longfellow, R.S. Lubna, S. Luitel, M. Madurga, R. Mahajan, M.J. Mogannam, C. Morse, S. Neupane, A. Nowicki, T.H. Ogunbeku, W.-J. Ong, C. Porzio, C.J. Prokop, B.C. Rasco, E.K. Ronning, E. Rubino, T.J. Ruland, K.P. Rykaczewski, L. Schaedig, D. Seweryniak, K. Siegl, M. Singh, S.L. Tabor, T.L. Tang, T. Wheeler, J.A. Winger, Z. Xu, Crossing N = 28 toward the neutron drip line: first measurement of half-lives at FRIB, Phys. Rev. Lett. 129 (21) (2022) 212501. https://doi.org/10.1103/PhysRevLett.129.212501

[12] H. Wolter, M. Colonna, D. Cozma, P. Danielewicz, C.M. Ko, R. Kumar, A. Ono, M.B. Tsang, J. Xu, Y.-X. Zhang, E. Bratkovskaya, Z.-Q. Feng, T. Gaitanos, A. Le Fèvre, N. Ikeno, Y. Kim, S. Mallik, P. Napolitani, D. Oliinychenko, T. Ogawa, M. Papa, J. Su, R. Wang, Y.-J. Wang, J. Weil, F.-S. Zhang, G.-Q. Zhang, Z. Zhang, J. Aichelin, W. Cassing, L.-W. Chen, H.-G. Cheng, H. Elfner, K. Gallmeister, C. Hartnack, S. Hashimoto,

S. Jeon, K. Kim, M. Kim, B.-A. Li, C.-H. Lee, Q.-F. Li, Z.-X. Li, U. Mosel, Y. Nara, K. Niita, A. Ohnishi, T. Sato, T. Song, A. Sorensen, N. Wang, W.-J. Xie, Transport model comparison studies of intermediate-energy heavy-ion collisions, Prog. Part. Nucl. Phys. 125 (2022) 103962. https://doi.org/10.1016/j.ppnp.2022.103962

[13] P. Danielewicz, R. Lacey, W.G. Lynch, Determination of the equation of state of dense matter, Science 298 (5598) (2002) 1592–1596. https://doi.org/10.1126/science.1078070

[14] Z. Kohley, L.W. May, S. Wuenschel, M. Colonna, M. Di Toro, M. Zielinska-Pfabe, K. Hagel, R. Tripathi, A. Bonasera, G.A. Souliotis, D.V. Shetty, S. Galanopoulos, M. Mehlman, W.B. Smith, S.N. Soisson, B.C. Stein, S.J. Yennello, Transverse collective flow and midrapidity emission of isotopically identified light charged particles, Phys. Rev. C 83 (4) (2011) 044601. https://doi.org/10.1103/PhysRevC.83.044601

[15] P. Russotto, P.Z. Wu, M. Zoric, M. Chartier, Y. Leifels, R.C. Lemmon, Q. Li, J. Łukasik, A. Pagano, P. Pawłowski, W. Trautmann, Symmetry energy from elliptic flow in ^{197}Au + ^{197}Au, Phys. Lett. B 697 (5) (2011) 471–476. https://doi.org/10.1016/j.physletb.2011.02.033

[16] A. Ono, H. Horiuchi, T. Maruyama, A. Ohnishi, Antisymmetrized version of molecular dynamics with two-nucleon collisions and its application to heavy ion reactions, Progr. Theor. Phys. 87 (5) (1992) 1185–1206. https://doi.org/10.1143/PTP/87.5.1185

[17] N. Ikeno, A. Ono, Collision integral with momentum-dependent potentials and its impact on pion production in heavy-ion collisions, Phys. Rev. C Nucl. Phys. 108 (4) (2023). https://doi.org/10.1103/physrevc.108.044601

[18] A. Ono, Cluster correlations in multifragmentation, J. Phys. Conf. Ser. 420 (1) (2013) 012103. https://doi.org/10.1088/1742-6596/420/1/012103

[19] J. Aichelin, A. Rosenhauer, G. Peilert, H. Stoecker, W. Greiner, Importance of momentum-dependent interactions for the extraction of the nuclear equation of state from high-energy heavy-ion collisions, Phys. Rev. Lett. 58 (19) (1987) 1926–1929. https://doi.org/10.1103/PhysRevLett.58.1926

[20] T. Kobayashi, N. Chiga, T. Isobe, Y. Kondo, T. Kubo, K. Kusaka, T. Motobayashi, T. Nakamura, J. Ohnishi, H. Okuno, H. Otsu, T. Sako, H. Sato, Y. Shimizu, K. Sekiguchi, K. Takahashi, R. Tanaka, K. Yoneda, SAMURAI Spectrometer for RI beam experiments, Nucl. Instrum. Methods Phys. Res. B 317 (2013) 294–304. https://doi.org/10.1016/j.nimb.2013.05.089

[21] H. Otsu, S. Koyama, N. Chiga, T. Isobe, T. Kobayashi, Y. Kondo, M. Kurokawa, W.G. Lynch, T. Motobayashi, T. Murakami, T. Nakamura, M. Kurata-Nishimura, V. Panin, H. Sato, Y. Shimizu, H. Sakurai, M.B. Tsang, K. Yoneda, H. Wang, SAMURAI in its operation phase for RIBF users, Nucl. Instrum. Methods Phys. Res. B 376 (2016) 175–179. https://doi.org/10.1016/j.nimb.2016.02.056

[22] T. Kubo, D. Kameda, H. Suzuki, N. Fukuda, H. Takeda, Y. Yanagisawa, M. Ohtake, K. Kusaka, K. Yoshida, N. Inabe, T. Ohnishi, A. Yoshida, K. Tanaka, Y. Mizoi, BigRIPS separator and zerodegree spectrometer at RIKEN RI beam factory, Prog. Theor. Exp. Phys. 2012 (1) (2012) 03C003. https://doi.org/10.1093/ptep/pts064

[23] R. Shane, A.B. McIntosh, T. Isobe, W.G. Lynch, H. Baba, J. Barney, Z. Chajecki, M. Chartier, J. Estee, M. Famiano, B. Hong, K. Ieki, G. Jhang, R. Lemmon, F. Lu, T. Murakami, N. Nakatsuka, M. Nishimura, R. Olsen, W. Powell, H. Sakurai, A. Taketani, S. Tangwancharoen, M.B. Tsang, T. Usukura, R. Wang, S.J. Yennello, J. Yurkon, SπRIT: a time-projection chamber for symmetry-energy studies, Nucl. Instrum. Methods Phys. Res. A 784 (2015) 513–517. https://doi.org/10.1016/j.nima.2015.01.026

[24] S. Tangwancharoen, W.G. Lynch, J. Barney, J. Estee, R. Shane, M.B. Tsang, Y. Zhang, T. Isobe, M. Kurata-Nishimura, T. Murakami, Z.G. Xiao, Y.F. Zhang, A gating grid driver for time projection chambers, Nucl. Instrum. Methods Phys. Res. A 853 (2017) 44–52. https://doi.org/10.1016/j.nima.2017.02.001

[25] T. Isobe, G. Jhang, H. Baba, J. Barney, P. Baron, G. Cerizza, J. Estee, M. Kaneko, M. Kurata-Nishimura, J.W. Lee, W.G. Lynch, T. Murakami, N. Nakatsuka, E.C. Pollacco, W. Powell, H. Sakurai, C. Santamaria, D. Suzuki, S. Tangwancharoen, M.B. Tsang, Application of the generic electronics for time projection chamber (GET) readout system for heavy radioactive isotope collision experiments, Nucl. Instrum. Methods Phys. Res. A 899 (2018) 43–48. https://doi.org/10.1016/j.nima.2018.05.022

[26] G. Jhang, J. Estee, J. Barney, G. Cerizza, M. Kaneko, J.W. Lee, W.G. Lynch, T. Isobe, M. Kurata-Nishimura, T. Murakami, Others, Symmetry energy investigation with pion production from sn + sn systems, Phys. Lett. B 813 (2021) 136016.

[27] J.W. Lee, G. Jhang, G. Cerizza, J. Barney, J. Estee, T. Isobe, M. Kaneko, M. Kurata-Nishimura, W.G. Lynch, T. Murakami, C.Y. Tsang, M.B. Tsang, R. Wang, B. Hong, A.B. McIntosh, H. Sakurai, C. Santamaria, R. Shane, S. Tangwancharoen, S.J. Yennello, Y. Zhang, Charged particle track reconstruction with SπRIT time projection chamber, Nucl. Instrum. Methods Phys. Res. A 965 (2020) 163840. https://doi.org/10.1016/j.nima.2020.163840

[28] M. Kaneko, T. Murakami, T. Isobe, M. Kurata-Nishimura, A. Ono, N. Ikeno, J. Barney, G. Cerizza, J. Estee, G. Jhang, J.W. Lee, W.G. Lynch, C. Santamaria, C.Y. Tsang, M.B. Tsang, R. Wang, D.S. Ahn, L. Atar, T. Aumann, H. Baba, K. Boretzky, J. Brzychczyk, N. Chiga, N. Fukuda, I. Gašparić, B. Hong, A. Horvat, T. Ichihara, K. Ieki, N. Inabe, Y.J. Kim, T. Kobayashi, Y. Kondo, P. Lasko, H.S. Lee, Y. Leifels, J. Łukasik, J. Manfredi, A.B. McIntosh, P. Morfouace, T. Nakamura, N. Nakatsuka, S. Nishimura, R. Olsen, H. Otsu, P. Pawłowski, K. Pelczar, D. Rossi, H. Sakurai, H. Sato, H. Scheit, R. Shane, Y. Shimizu, H. Simon, T. Sumikama, D. Suzuki, H. Suzuki, H. Takeda, S. Tangwancharoen, Y. Togano, H. Törnqvist, Z. Xiao, S.J. Yennello, J. Yurkon, Y. Zhang, Rapidity distributions of $Z = 1$ isotopes and the nuclear symmetry energy from Sn + Sn collisions with radioactive beams at 270 MeV/nucleon, Phys. Lett. B 822 (136681) (2021) 136681. https://doi.org/10.1016/j.physletb.2021.136681

[29] J.W. Lee, M.B. Tsang, C.Y. Tsang, R. Wang, J. Barney, J. Estee, T. Isobe, M. Kaneko, M. Kurata-Nishimura, W.G. Lynch, T. Murakami, A. Ono, S.R. Souza, D.S. Ahn, L. Atar, T. Aumann, H. Baba, K. Boretzky, J. Brzychczyk, G. Cerizza, N. Chiga, N. Fukuda, I. Gasparic, B. Hong, A. Horvat, K. Ieki, N. Ikeno, N. Inabe, G. Jhang, Y.J. Kim, T. Kobayashi, Y. Kondo, P. Lasko, H.S. Lee, Y. Leifels, J. Łukasik, J. Manfredi, A.B. McIntosh, P. Morfouace, T. Nakamura, N. Nakatsuka, S. Nishimura, H. Otsu, P. Pawłowski, K. Pelczar, D. Rossi, H. Sakurai, C. Santamaria, H. Sato, H. Scheit, R. Shane, Y. Shimizu, H. Simon, A. Snoch, A. Sochocka, T. Sumikama, H. Suzuki, D. Suzuki, H. Takeda, S. Tangwancharoen, Y. Togano, Z.G. Xiao, S.J. Yennello, Y. Zhang, (the S π RIT collaboration), Isoscaling in central Sn + Sn collisions at 270 MeV/u, Eur. Phys. J. A 58 (2022) 201. https://doi.org/10.1140/epja/s10050-022-00851-2

[30] J. Estee, W.G. Lynch, J. Barney, G. Cerizza, G. Jhang, J.W. Lee, R. Wang, T. Isobe, M. Kaneko, M. Kurata-Nishimura, T. Murakami, R. Shane, S. Tangwancharoen, C.Y. Tsang, M.B. Tsang, B. Hong, P. Lasko, J. Łukasik, A.B. McIntosh, P. Pawłowski, K. Pelczar, H. Sakurai, C. Santamaria, D. Suzuki, S.J. Yennello, Y. Zhang, Extending the dynamic range of electronics in a time projection chamber, Nucl. Instrum. Methods Phys. Res. A 944 (2019) 162509. https://doi.org/10.1016/j.nima.2019.162509

[31] C.Y. Tsang, J. Estee, R. Wang, J. Barney, G. Jhang, W.G. Lynch, Z.Q. Zhang, G. Cerizza, T. Isobe, M. Kaneko, M. Kurata-Nishimura, J.W. Lee, T. Murakami, M.B. Tsang, Space charge effects in the SπRIT time projection chamber, Nucl. Instrum. Methods Phys. Res. A 959 (2020) 163477. https://doi.org/10.1016/j.nima.2020.163477

[32] N. Ikeno, A. Ono, Y. Nara, A. Ohnishi, Probing neutron-proton dynamics by pions, Phys. Rev. C 93 (4) (2016) 044612. https://doi.org/10.1103/PhysRevC.93.044612

[33] A. Ono, Dynamics of clusters and fragments in heavy-ion collisions, Prog. Part. Nucl. Phys. 105 (2019) 139–179. https://doi.org/10.1013/j.ppnp.2018.11.001

[34] E. Chabanat a, R. Bonche b, R. Haensel c, J. Meyer a, R. Schaeffer b, A skyrme parametrization from subnuclear to neutron star densities. Part II. Nuclei far from stabilities, Nucl. Phys. A 635 (1998) 231–256. https://doi.org/10.1016/S0375-9474(98)00180-8

[35] E. Chabanat, P. Bonche, P. Haensel, J. Meyer, R. Schaeffer, Erratum to "A Skyrme parametrization from subnuclear to neutron star densities. (II)" Nuclei far from stabilities" <upper-case>[Nucl. Phys. A 635 (1998) 231-256]</upper-case> *, Nucl. Phys. A 643 (1–2) (1998) 441. https://doi.org/10.1016/s0375-9474(98)00570-3

[36] S. Hama, B.C. Clark, E.D. Cooper, H.S. Sherif, R.L. Mercer, Global Dirac optical potentials for elastic proton scattering from heavy nuclei, Phys. Rev. C 41 (6) (1990) 2737–2755. https://doi.org/10.1103/physrevc.41.2737

[37] C. Gale, G. Bertsch, Das Gupta S, Heavy-ion collision theory with momentum-dependent interactions, Phys. Rev. C 35 (5) (1987) 1666–1671. https://doi.org/10.1103/physrevc.35.1666

[38] W. Reisdorf, A. Andronic, A. Gobbi, O.N. Hartmann, N. Herrmann, K.D. Hildenbrand, Y.J. Kim, M. Kirejczyk, P. Koczoń, T. Kress, Y. Leifels, A. Schüttauf, Z. Tymiński, Z.G. Xiao, J.P. Alard, V. Barret, Z. Basrak, N. Bastid, M.L. Benabderrahmane, R. Caplar, P. Crochet, P. Dupieux, M. Dzelalija, Z. Fodor, Y. Grishkin, B. Hong, J. Kecskemeti, M. Korolija, R. Kotte, A. Lebedev, X. Lopez, M. Merschmeyer, J. Mösner, W. Neubert, D. Pelte, M. Petrovici, F. Rami, B. de Schauenburg, Z. Seres, B. Sikora, K.S. Sim, V. Simion, K. Siwek-Wilczyńska, V. Smolyankin, M. Stockmeier, G. Stoicea, P. Wagner, K. Wiśniewski, D. Wohlfarth, I. Yushmanov, A. Zhilin, FOPI Collaboration, Nuclear stopping from 0.09A to 1.93A GeV and its correlation to flow, Phys. Rev. Lett. 92 (23) (2004) 232301. https://doi.org/10.1103/PhysRevLett.92.232301

[39] A.M. Poskanzer, S.A. Voloshin, Methods for analyzing anisotropic flow in relativistic nuclear collisions, Phys. Rev. C 58 (3) (1998) 1671–1678. https://doi.org/10.1103/PhysRevC.58.1671

[40] J. Barrette, R. Bellwied, S. Bennett, R. Bersch, P. Braun-Munzinger, W.C. Chang, W.E. Cleland, M. Clemen, J. Cole, T.M. Cormier, Y. Dai, G. David, J. Dee, O. Dietzsch, M. Drigert, K. Filimonov, S.C. Johnson, J.R. Hall, T.K. Hemmick, N. Herrmann, B. Hong, Y. Kwon, R. Lacasse, Q. Li, T.W. Ludlam, S.K. Mark, R. Matheus, S. McCorkle, J.T. Murgatroyd, D. Miśkowiec, E. O'Brien, S. Panitkin, T. Piazza, M. Pollack, C. Pruneau, M.N. Rao, E. Reber, M. Rosati, N.C. da Silva, S. Sedykh, U. Sonnadara, J. Stachel, E.M. Takagui, S. Voloshin, T.B. Vongpaseuth, G. Wang, J.P. Wessels, C.L. Woody, N. Xu, Y. Zhang, C. Zou, Proton and pion production relative to the reaction plane in Au + Au collisions at 11AGeV/c, Phys. Rev. C 56 (6) (1997) 3254–3264. https://doi.org/10.1103/physrevc.56.3254

[41] W. Reisdorf, Y. Leifels, A. Andronic, R. Averbeck, V. Barret, Z. Basrak, N. Bastid, M.L. Benabderrahmane, R. Čaplar, P. Crochet, P. Dupieux, M. Dželalija, Z. Fodor, P. Gasik, Y. Grishkin, O.N. Hartmann, N. Herrmann, K.D. Hildenbrand, B. Hong, T.I. Kang, J. Kecskemeti, Y.J. Kim, M. Kirejczyk, M. Kiš, P. Koczoń, M. Korolija, R. Kotte, T. Kress, A. Lebedev, X. Lopez, T. Matulewicz, M. Merschmeyer, W. Neubert, M. Petrovici, K. Piasecki, F. Rami, M.S. Ryu, A. Schüttauf, Z. Seres, B. Sikora, K.S. Sim, V. Simion, K. Siwek-Wilczyńska, V. Smolyankin, M. Stockmeier, G. Stoicea, Z. Tymiński, K. Wiśniewski, D. Wohlfarth, Z.G. Xiao, H.S. Xu, I. Yushmanov, A. Zhilin, Systematics of azimuthal asymmetries in heavy ion collisions in the 1A GeV regime, Nucl. Phys. A 876 (2012) 1–60. https://doi.org/10.1016/j.nuclphysa.2011.12.006

[42] A. Andronic, V. Barret, Z. Basrak, N. Bastid, L. Benabderrahmane, G. Berek, R. Čaplar, E. Cordier, P. Crochet, P. Dupieux, M. Dželalija, Z. Fodor, I. Gasparic, Y. Grishkin, O.N. Hartmann, N. Herrmann, K.D. Hildenbrand, B. Hong, J. Kecskemeti, Y.J. Kim, M. Kirejczyk, P. Koczon, M. Korolija, R. Kotte, T. Kress, A. Lebedev, Y. Leifels, X. Lopez, A. Mangiarotti, M. Merschmeyer, W. Neubert, D. Pelte, M. Petrovici, F. Rami, W. Reisdorf, B. de Schauenburg, A. Schüttauf, Z. Seres, B. Sikora, K.S. Sim, V. Simion, K. Siwek-Wilczyńska, V. Smolyankin, M.R. Stockmeier, G. Stoicea, Z. Tyminski, P. Wagner, K. Wiśniewski, D. Wohlfarth, Z.-G. Xiao, I. Yushmanov, A. Zhilin, Excitation function of elliptic flow in Au + Au collisions and the nuclear matter equation of state, Phys. Lett. B 612 (3–4) (2005) 173–180. https://doi.org/10.1016/j.physletb.2005.02.060